The Roles of TNFR1 in Lipopolysaccharide-Induced Bone Loss: Dual Effects of TNFR1 on Bone Metabolism via Osteoclastogenesis and Osteoblast Survival

Hiroki Ochi,[1] Yasushi Hara,[1] Masahiro Tagawa,[1] Kenichi Shinomiya,[2] Yoshinari Asou[2]

[1]Division of Veterinary Surgery, Department of Veterinary Science, Faculty of Veterinary Medicine, Nippon Veterinary and Life Science University, 1-7-1 Kyonan-cho, Musashino, Tokyo, Japan, [2]Department of Orthopaedics Surgery, Tokyo Medical and Dental University, 1-5-45 yushima bunkyo-ku, Tokyo, 13-8519, Japan

Received 30 May 2009; accepted 10 September 2009
Published online 4 November 2009 in Wiley InterScience (www.interscience.wiley.com). DOI 10.1002/jor.21028

ABSTRACT: LPS (lipopolysaccharide), a major constituent of Gram-negative bacteria, regulates proliferation and differentiation of osteoclasts directly or indirectly. This study sought to investigate the functions of the RANK/RANKL pathway in LPS-induced bone loss in vivo. Wild-type mice or TNFR1−/− mice were injected LPS with or without osteoprotegerin (OPG) and analyzed histologically. Bone volume was reduced by LPS injection in all groups, and OPG administration prevented the LPS-induced bone loss regardless of genotypes. LPS-induced enhancement of osteoclastogenesis in wild-type mice was blocked by OPG administration. LPS or OPG did not affect osteoclastogenesis in TNFR1−/− mice. Interestingly, osteoblast surface was remarkably reduced in LPS-treated TNFR1−/− mice as a result of enhanced osteoblast apoptosis. TRAIL, induced by TNF-α in BMC, triggered apoptosis of primary osteoblast only when TNFR1 signal was ablated in vitro. In conclusion, RANK signaling plays a prominent role in osteoclastogenesis downstream of LPS. Furthermore, TNFR1 regulates bone metabolism through not only the regulation of osteoclast differentiation but also osteoblast survival. © 2009 Orthopaedic Research Society. Published by Wiley Periodicals, Inc. J Orthop Res 28:657–663, 2010

Keywords: lipopolysaccharide; osteoprotegerin; TNFR1; osteoclast; osteoblast

Bacterial infections are associated with rapid bone destruction in osteomyelitis, bacterial arthritis, and infected orthopedic implant failure.[1,2] Lipopolysaccharide (LPS), a major constituent of Gram-negative bacteria, is one of the molecular factors plays a major role in bone resorption in periodontitis or ostemyelitis [1] by stimulating the the production of proinflammatory cytokines.[3,4] LPS stimulates synthesis of tumor necrosis factor-α (TNF-α), via NF-κB activation.[5,6] At the cellular level, TNF-α affects bone structure through the inhibition of osteoblast function and stimulation of osteoclast formation both directly and indirectly.[7–9] TNF-α directly targets osteoclasts and their precursors, and that deletion of its type-1 receptor (TNFR1) lessens osteoclastogenesis and impacts RANK signaling molecules.[9,10] LPS injection induces osteoclastogenesis via TNF-α ligation of TNFR1 in vivo.[10,11] Therefore, TNF-α can be considered to be a critical link between chronic inflammation and bone loss. Receptor activator of NF-κB ligand (RANKL) was identified as an essential factor in osteoclastogenesis.[12,13] Osteoblasts/stromal cells produce a soluble decoy receptor for RANKL, osteoprotegerin (OPG), which interrupts the interaction between RANKL and RANK to inhibit osteoclast formation both in vivo and in vitro.[12,14] LPS enhance RANKL production and suppress OPG production from osteoblasts in vitro.[15–17] Moreover, LPS can enhance the survival, fusion, and activation of osteoclasts independent of IL-1, TNF-α, and RANKL.[18] Thus, osteoclastogenesis is regulated by variety of signaling pathways downstream of LPS. However, it remains to be well understood which pathways are prominent in vivo. This study sought to investigate the relative importance of the direct effect of LPS, RANK/RANKL-mediated pathway and TNF-α/TNFR1-mediated pathway in LPS-induced bone loss in vivo.

Correspondence to: Yoshinari Asou (T: +81-3-5803-5279; F: +81-3-5803-5281; E-mail: aso.orth@tmd.ac.jp)

MATERIALS AND METHODS

Mice

Male wild-type or TNFR1−/− mice on the C57BL/6 background were obtained from Jackson Laboratory (Bar Harbor, ME, USA). All studies were approved by the institutional animal care committee.

Histological Analysis

Male mice (6–8 months, $n = 5–7$) were injected with 20 mg/kg body weight LPS (Sigma, St. Louis, MO, USA) or phosphate-buffered saline (PBS) subcutaneously on day 0. PBS or recombinant human OPG (Sankyo-Daiichi Co., Ltd., Tokyo, Japan) was given intraperitoneally on day 0 and day 1. All mice were sacrificed 48 h after LPS injection. Tibiae of each mouse were fixed in 4% paraformaldehyde for decalcified samples or in 70% ethanol for undecalcified samples. For decalcification, samples were treated with EDTA, dehydrated, and embedded in paraffin, then sectioned at a 6-μm thickness. Undecalcified samples were dehydrated, embedded in glycol metacrylate, sectioned, and stained for TRAP activity and ALP activity. Trabecular bone of the tibiae 200 to 600 μm away from growth plate was evaluated for histomorphometry using an image analyzer (Image pro plus, Planetron Inc., Tokyo, Japan). The abbreviations for histomorphometric parameters were according to the recommendation by the American Society of Bone and Mineral Research Histomorphometry Nomenclature Committee.[19]

Flow Cytometry Analysis

Bone marrow cells were isolated from the bone marrow by flushing with culture medium using a 21-gauge needle. Bone

marrow cells were incubated for 30 min with a FITC-conjugated monoclonal antimouse antibody against CD11b or Phycoerythrin-conjugated monoclonal antimouse antibody against TRAIL (eBioscience, San Diego, CA, USA). After washing in PBS, cells were diluted in 1 mL 1% paraformaldehyde and subjected to FACS analysis. Samples were analyzed using a FACScan flow cytometer (BD Biosciences, Franklin Lakes, NJ, USA).

Culture of Primary Mouse Osteoblastic Cells

Primary osteoblastic cells were isolated from 1-day-old mouse calvariae after five routine sequential digestions with 0.1% collagenase (Wako, Tokyo, Japan) and 0.2% dispase (Godo Shusei, Tokyo, Japan) as previously described.[20] Osteoblastic cells were combined and cultured at 37°C in α-MEM supplemented with 10% FCS under 5% CO_2 in air.

Terminal Deoxynucleotidyltransferase-Mediated UTP End Labeling (TUNEL) Assay

TUNEL assays were conducted using decalcified sections of femoral bones according to the manufacturer's instruction (TaKaRa, Tokyo, Japan). The number of TUNEL-positive cells was quantitated in the femoral bone marrow of paraffin-embedded samples.

Measurement of Cellular Injury

Primary osteoblasts (3×10^3 cells/dish), plated in 100 μL α-MEM supplemented with 10% FBS, were incubated at 37°C in 96-well dishes. After 2 days of culture, the medium was changed to 100 μL α-MEM supplemented with 10% FBS. Subsequently, cells were treated with TRAIL (Sigma) or Tween20, for positive control. After 24 h of culture, cellular injury was quantitated by the measurement of lactate dehydrogenase (LDH) release using an LDH-cytotoxicity assay kit (WAKO, Tokyo, Japan).

Measurement of Caspase Activity

Primary osteoblasts (3×10^6 cells/10-cm dish), plated in 100 μL α-MEM supplemented with 10% FBS, were incubated at 37°C. After 2 days of culture, the medium was changed to 100 μL α-MEM supplemented with 10% FBS. Subsequently, cells were treated with TRAIL for 6 hours (100 ng/mL, Sigma) or vehicle, for negative control. Caspase3 activity was quantified by caspase colorimetric assay kit (Clontech, Palo Alto, CA, USA). Representative set of results was selected from three independent experiments for display.

RESULTS

LPS-induced bone reduction was ameliorated by OPG administration. LPS stimulates bone resorption in vivo. To examine the effect of OPG on LPS-induced bone resorption, wild-type mice were injected with LPS in the presence or absence of OPG. Following sacrifice 48 h after injection, LPS treatment reduced BV/TV approximately 40% in the proximal region of tibial bones in wild-type mice (Fig. 1a). OPG administration reversed the LPS-induced bone loss in a dose-dependent manner. OPG administration at a dose of 0.5 mg/kg was sufficient to maintain bone volume within basal levels (Fig. 1a). As LPS treatment induces osteoclastogenesis through a TNFR1-dependent pathway,[10] TNFR1−/− mice were also injected with LPS in the presence or absence of OPG to investigate the roles of TNF-α and RANKL in LPS-induced osteoclastogenesis. TNF-α mRNA expression levels of bone marrow cells in wild-type and TNFR1−/− mice were similary enhanced 1 h after LPS injection (data not shown). Histomorphometric analysis, however, indicated that BV/TV was significantly reduced in LPS-injected TNFR1−/− mice (Fig. 1b). The reduction in bone volume was partially reversed by OPG treatment (Fig. 1b), but not significantly.

LPS Enhancement of Osteoclastogenesis Through TNFR1 and RANK Pathways

Histological analysis revealed Oc.S/BS and N.Oc/BS were increased in LPS-treated wild-type mice (Fig. 2b, g, and h). OPG treatment suppressed the observed LPS-induced osteoclastogenesis in a dose-dependent manner (Fig. 2g and h). Treatment with 0.5 mg/kg OPG completely reversed the changes in N.Oc/BS, returning these values to basal levels (Fig. 2g and h). In contrast, LPS and OPG had little effect on N.Oc/BS and Oc.S/BS

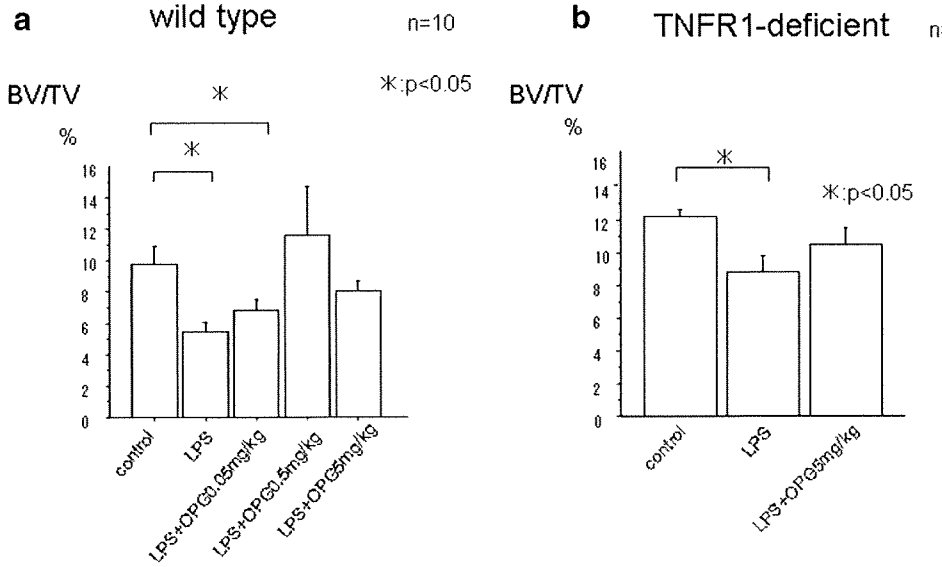

Figure 1. Histological analysis (a, b) indicated that the trabecular bone volume was significantly reduced in both wild-type (a) and TNFR1−/− (b) mice. Also, OPG administration inhibited the LPS-induced bone loss in wild-type animals in a dose-dependent manner (a), and bone volume was partially rescued by OPG injection in TNFR1−/− mice (b). Bars, ±SD. *$p < 0.05$ compared with control. Asterisk indicates statistically significant difference ($p < 0.05$).

in TNFR1−/− mice in comparison with wild-type mice (Fig. 2d–f, j, and k). Although urinary deoxypyridinoline, a marker for bone resorption, was increased the day after LPS injection in wild-type mice (Fig. 2i), these levels were unaffected by LPS or OPG treatment of TNFR1−/− mice (Fig. 2l). These results indicated TNFR1-mediated RANK/RANKL signaling plays a dominant role in LPS-induced osteoclastogenesis and osteoclastic bone resorption. To investigate the effect of TNFR1 and OPG on osteoclast precursors in the bone marrow, bone marrow cells were analyzed by flow cytometry. Two days after LPS injection (20 mg/kg), the numbers of CD11b-positive osteoclast precursors were increased in wild-type mice (Fig. 3a and b). In contrast, the population of CD11b-positive cells in the bone marrow of TNFR1−/− mice was not affected by LPS injection (Fig. 3d and e), indicating that TNFR1-mediated signaling is necessary for LPS-induced enhancement of the osteoclast precursor population in the bone marrow. OPG injection (5 mg/kg) did not affect the composition of the CD11b-positive cell population, regardless of genotype (Fig. 3c and f), indicating that RANK/RANKL signaling plays a role in osteoclast differentiation, rather than regulation of the osteoclast precursor population.

LPS Treatment-Induced High Turnover Osteopenia in Wild-Type Mice, but Low Turnover Levels in TNFR1-Deficient Mice

Next, we investigated the effect of LPS on bone formation. Forty-eight hours after LPS injection, the ALP-positive area and Ob.S/BS was increased as a result of high turnover osteopenia in wild-type mice (Figs. 2 and 4a). OPG treatment reduced these parameters to basal levels (Fig. 4a). In contrast, the ALP-positive area and Ob.S/BS were remarkably reduced in LPS-treated TNFR1−/− mice (Figs. 2 and 4c). Although serum osteocalcin levels were increased in wild-type mice immediately after LPS administration (Fig. 4b), the enhancement of osteocalcin levels was attenuated by in TNFR1−/− deficiency (Fig. 4d). Thus, TNFR1-mediated signaling was indispensable for the transient enhancement of bone formation during the acute phase of inflammation.

Susceptibility for TRAIL Was Induced by TNFR1-Deficiency in Murine Osteoblast

To address the mechanisms governing the reduction in osteoblasts in LPS-treated TNFR1−/− mice, we investigated the effect of LPS on osteoblast survival. TUNEL-positive cells were abundantly observed on the surface

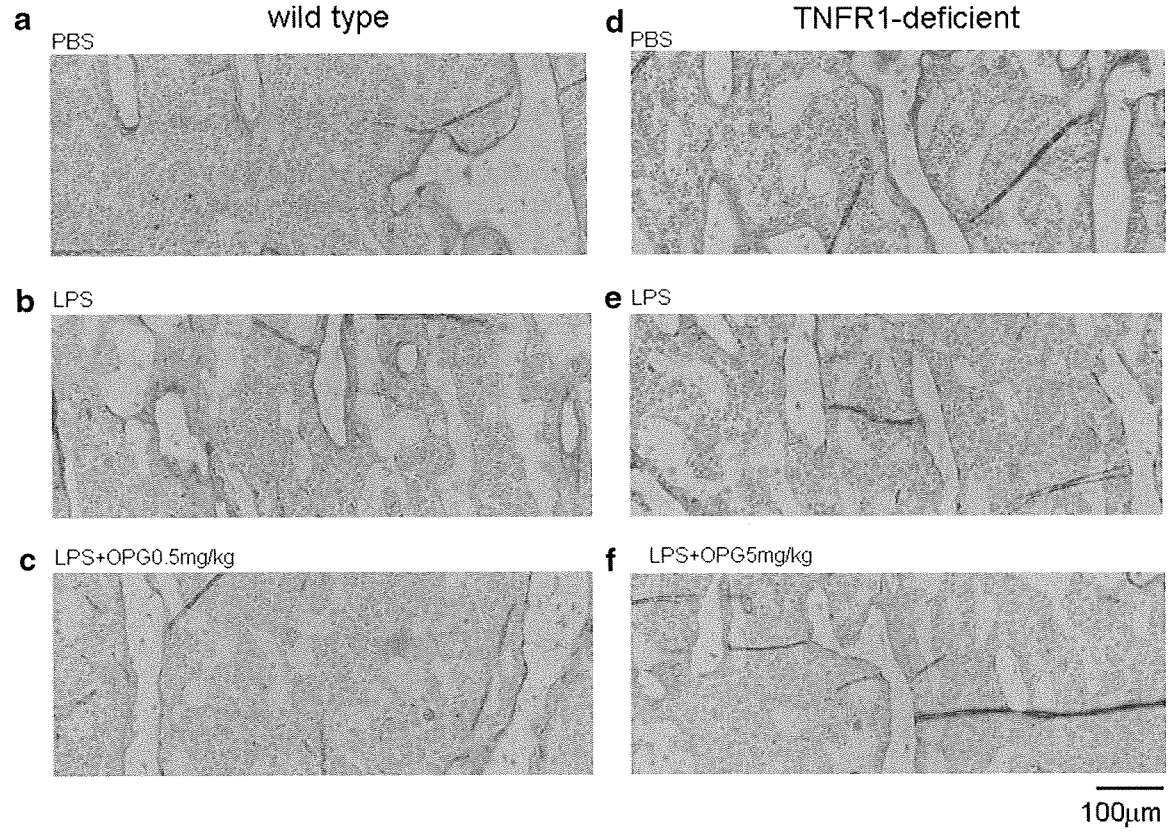

Figure 2. LPS injection induced high turnover osteopenia in wild-type mice and low turnover osteopenia in TNFR1−/− mice. Sections of tibiae from wild-type (a–c) and TNFR1−/− (d–f) mice were stained for TRAP activity (stained red) and ALP activity (stained purple). Osteoclast number was increased only in LPS-injected wild-type mice (b). ALP-positive area was also increased in LPS-treated wild-type mice (b), but decreased in LPS-treated TNFR1−/− mice (e, f). Both Oc.S/BS and N.Oc/BS were significantly increased in LPS-treated wild-type mice (g, h). OPG treatment suppressed the LPS-induced osteoclastogenesis in a dose-dependent manner (g, h). LPS or OPG had little effect on N.Oc/BS and Oc.S/BS in TNFR1−/− mice (j, k). Urinary deoxypyridinoline was increased on the day after LPS injection in wild-type mice only (i, l). Bars, ±SD. Asterisk indicates statistically significant difference ($p < 0.05$).

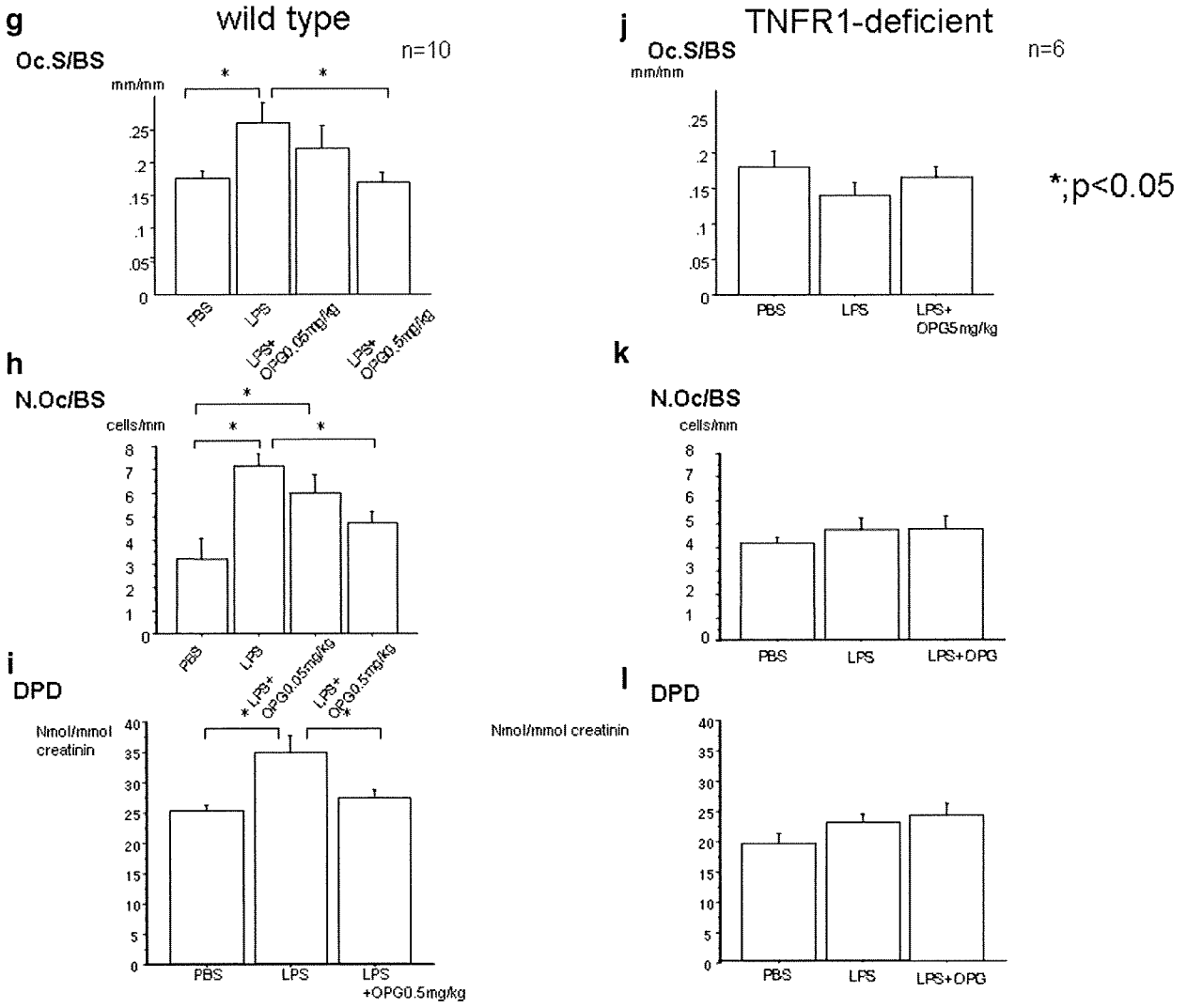

Figure 2. *(Continued)*

of the trabecular bone in LPS-treated TNFR1−/− mice (Fig. 5d and f), but not that in wild-type mice (Fig. 5c and f). LPS can induce secretion of soluble TRAIL (TNF-related apoptosis-inducing ligand), a member of the TNF cytokine family, in T cells, B cells, and monocytes.[21,22] Flow cytometry analysis revealed the population of TRAIL expressed bone marrow cells was increased by LPS injection in both wild-type and TNFR1−/− mice (Fig. 5e). An LDH assay of murine primary osteoblasts revealed TRAIL-induced osteoblast apoptosis was observed only in TNFRI−/− osteoblasts (g). TRAIL-induced caspase3 activity was enhanced in TNFR1−/− osteoblasts compared to wild type (h). Thus, susceptibility for TRAIL was induced by TNFR1-deficiency in murine osteoblast.

DISCUSSION

In this article, we demonstrate that OPG injection completely suppressed LPS-induced high turnover osteopenia via suppression of osteoclastogenesis. This result suggests that RANK signaling, not direct effect of LPS or TNF-α, plays a prominent role in osteoclastogenesis downstream of LPS. Furthermore, LPS-induced osteoclastogenesis was also suppressed by TNFR1-deficiency regardless of OPG injection, indicating that TNFR1 signaling was also indispensable for osteoclastogenesis, likely functioning upstream of RANK signaling.

Our flow cytometry analysis indicated that CD11b-positive osteoclast precursors increased after LPS injection of wild-type mice; this effect, however, was abolished by TNFR1 deficiency. Moreover, OPG injection had no effect on the population of CD11b-positive cells in the bone marrow. Previous reports of TNF-Tg mice revealed that osteoclast precursor (OCPs) numbers are increased four- to sevenfold in peripheral bone marrow cells.[23] RANK signaling is essential for terminal osteoclast differentiation in TNF-α-mediated inflammatory arthritis but not for the TNF-α-induced increase in OCPs.[24] These results are consistant with our study, indicating that TNF-α acts in the regulation of OCP population after LPS injection.

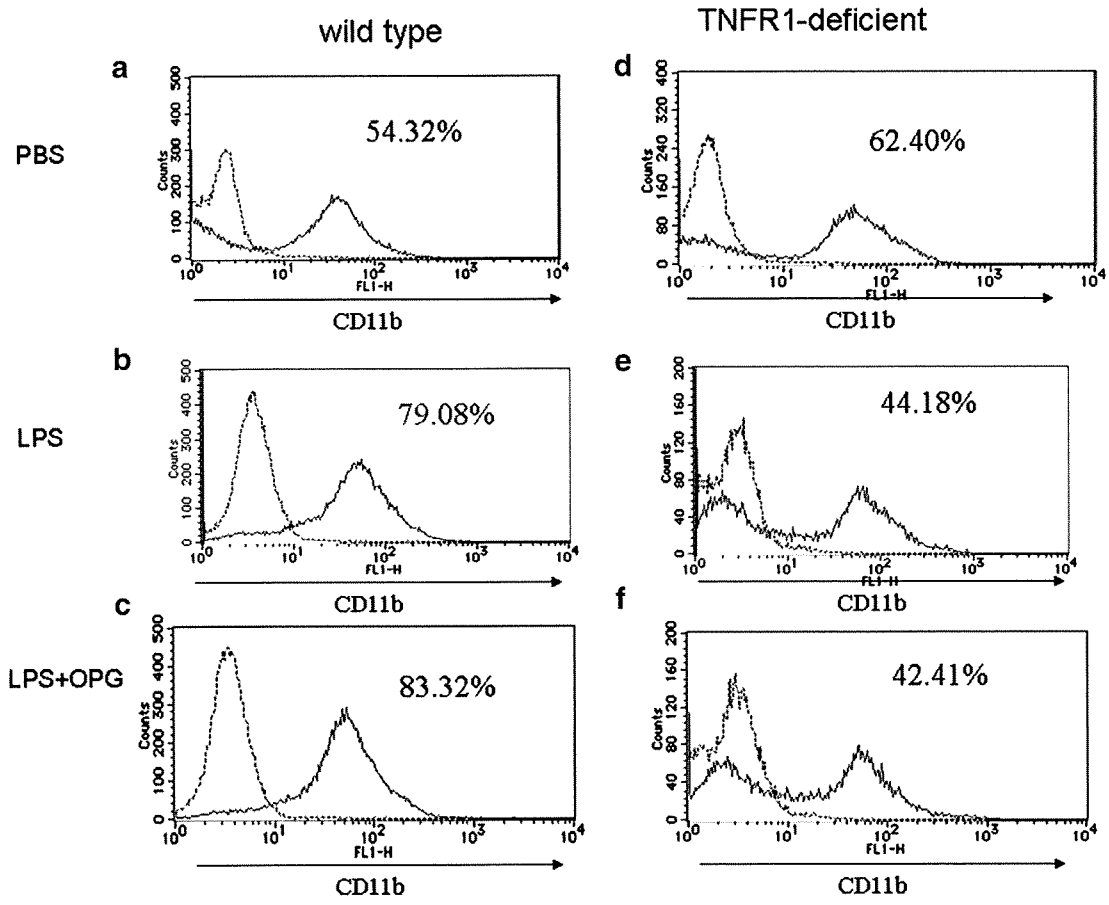

Figure 3. LPS injection increased the number of CD11b-positive bone marrow cells in wild-type, but not in TNFR1−/− mice. Bone marrow cells were analyzed by flow cytometry 2 days after LPS injection. The numbers of CD11b-positive osteoclast precursors were increased by LPS treatment only in wild-type mice. OPG injection did not affect the bone marrow CD11b-positive population (c, f).

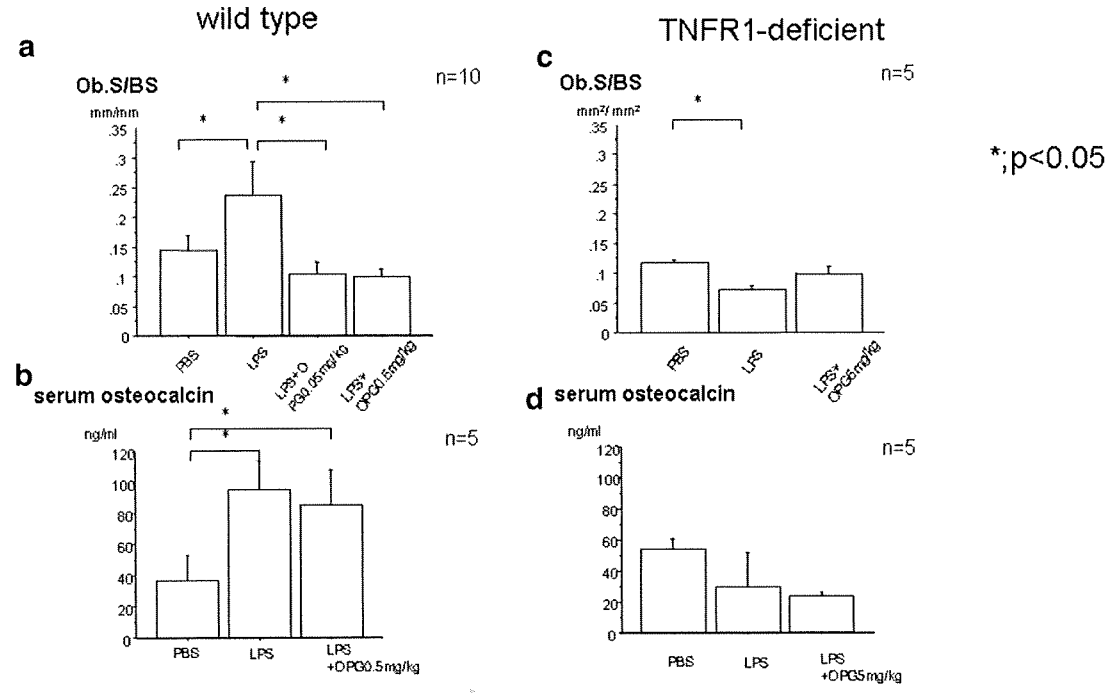

Figure 4. Bone formation activity was enhanced by in LPS-injected wild type mice, but not in TNFR1−/− mice. Ob.S/BS was increased LPS injection in wild-type mice following (a) but not in TNFR1−/− mice (c). OPG treatment reduced enhanced Ob.S/BS in wild-type mice to basal levels (a). In contrast, OPG had little effect on Ob.S/BS in TNFR1-deficient animals (d). Serum osteocalcin levels increased in wild-type mice (b), but not in TNFR1−/− mice (d) after LPS administration. Bars, ±SD. Asterisk indicates statistically significant difference ($p < 0.05$).

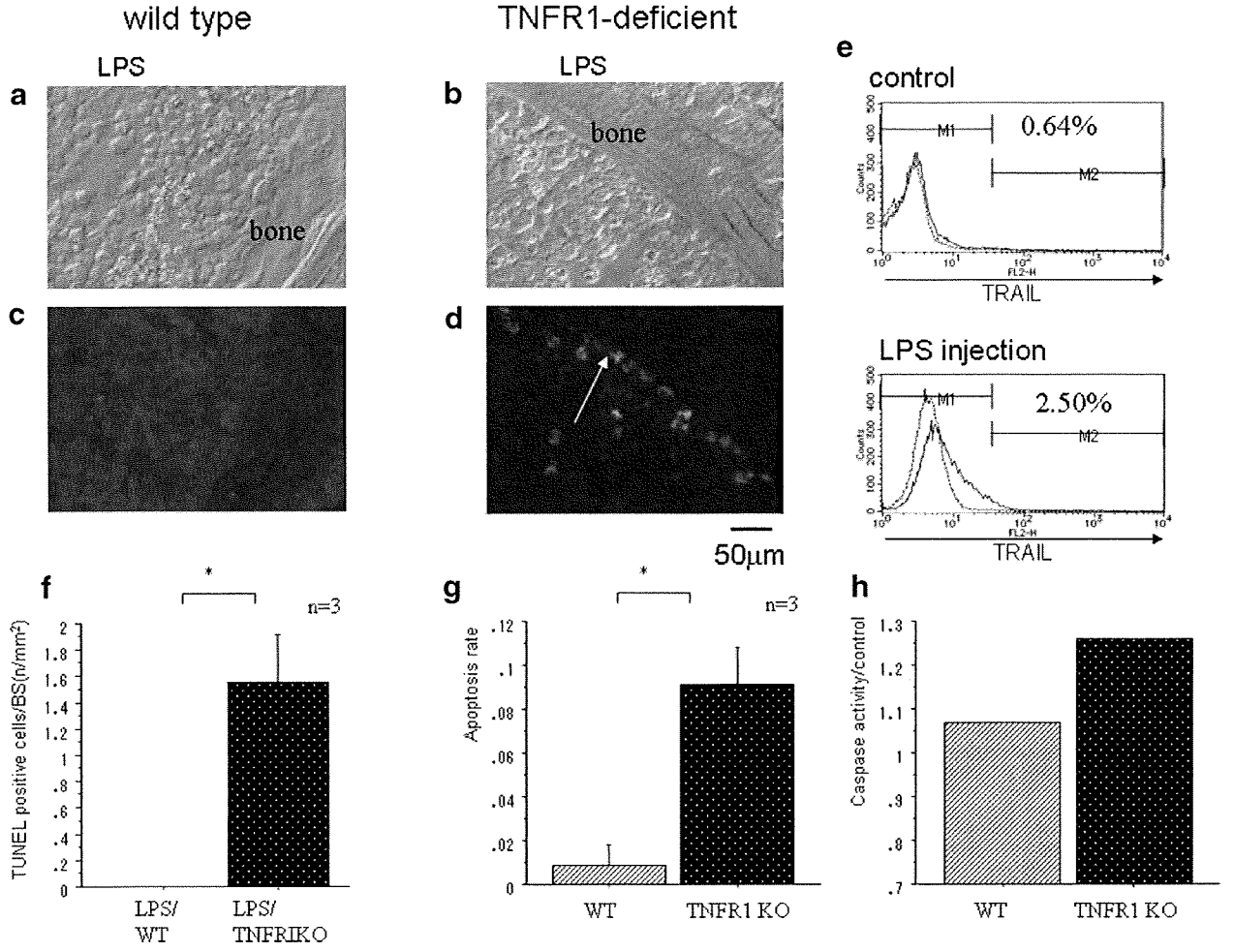

Figure 5. The numbers of TUNEL-positive cells increased on the surface of bones from LPS-injected TNFR1−/− mice. Sections were examined by TUNEL staining using bright-field (a, b) and dark-field (c, d) microscopy. TUNEL-positive cells were observed on the surface of trabecular bones from LPS-injected TNFR1−/− mice (e), but not those from wild-type mice (d). (c) Flow cytometry analysis of mouse bone marrow cells. TRAIL expressed cells were increased after LPS injection in wild-type mice (e). An LDH assay of murine primary osteoblasts indicated TRAIL-induced osteoblast apoptosis was enhanced by TNFRI deficiency (g). TRAIL-induced caspase3 activity was augmented in TNFR1−/− osteoblasts compared to wild type (h). Bars, ±SD. Asterisk indicates statistically significant difference ($p < 0.05$).

Interestingly, LPS injection induced low turnover osteopenia in TNFR1−/− mice. Enhanced osteoblast apoptosis contributed, at least partly, to this phenomenon. The remarkable reduction in Ob.S/BS and ALP-positive area in LPS-treated TNFR1−/− mice indicated that TNFR1 signaling plays a critical role in the maintenance of osteoblast numbers and function in LPS-mediated inflammation. As far as we know, this is the first paper to demonstrate a TNFR1-dependent anti-apoptotic effect of TNF-α on osteoblasts in vivo. Recently, TNFR1 was shown to promote cell survival via activation of NF-κB signal.[25] Meanwhile, serum-starved human microvascular endothelial cells (HMECs) plated on osteopontin are protected from cell death induced by TRAIL through $\alpha v\beta_3$ integrin ligation, downstream activation of NF-κB, and subsequent upregulation of OPG.[26] These data encouraged us to investigate the effect of TRAIL on osteoblast, whereas human osteoblast is resistant to TRAIL-mediated apoptosis.[27,28] As expected, TRAIL could induce apoptosis on TNFR1 deficient primary osteoblasts.

In conclusion, our data suggest that OPG can rescue the bone loss induced by LPS administration. These results indicate that OPG may be an effective tool for the treatment of human abnormal bone loss induced by LPS in diseases such as osteomyelitis or periodontitis. Furthermore, the osteopenia observed in inflammatory diseases including rheumatoid arthritis may be cured by the administration of OPG.

ACKNOWLEDGMENTS

This study was supported by Daiichi Sankyo Co., Ltd. All authors have no conflict of interest.

REFERENCES

1. Nair SP, Meghji S, Wilson M, et al. 1996. Bacterially induced bone destruction: mechanisms and misconceptions. Infect Immun 64:2371–2380.

2. Nair S, Song Y, Meghji S, et al. 1995. Surface-associated proteins from Staphylococcus aureus demonstrate potent bone resorbing activity. J Bone Miner Res 10:726–734.
3. Ulevitch RJ, Tobias PS. 1995. Receptor-dependent mechanisms of cell stimulation by bacterial endotoxin. Annu Rev Immunol 13:437–457.
4. Hla T, Lee MJ, Ancellin N, et al. 2001. Lysophospholipids—receptor revelations. Science 294:1875–1878.
5. Akira S, Takeda K. 2004. Toll-like receptor signalling. Nat Rev Immunol 4:499–511.
6. Lin SK, Kok SH, Kuo MY, et al. 2003. Nitric oxide promotes infectious bone resorption by enhancing cytokine-stimulated interstitial collagenase synthesis in osteoblasts. J Bone Miner Res 18:39–46.
7. Bertolini DR, Nedwin GE, Bringman TS, et al. 1986. Stimulation of bone resorption and inhibition of bone formation in vitro by human tumour necrosis factors. Nature 319:516–518.
8. Lam J, Takeshita S, Barker JE, et al. 2000. TNF-alpha induces osteoclastogenesis by direct stimulation of macrophages exposed to permissive levels of RANK ligand. J Clin Invest 106:1481–1488.
9. Zhang YH, Heulsmann A, Tondravi MM, et al. 2001. Tumor necrosis factor-alpha (TNF) stimulates RANKL-induced osteoclastogenesis via coupling of TNF type 1 receptor and RANK signaling pathways. J Biol Chem 276:563–568.
10. Abu-Amer Y, Ross FP, Edwards J, et al. 1997. Lipopolysaccharide-stimulated osteoclastogenesis is mediated by tumor necrosis factor via its P55 receptor. J Clin Invest 100:1557–1565.
11. Kobayashi K, Takahashi N, Jimi E, et al. 2000. Tumor necrosis factor alpha stimulates osteoclast differentiation by a mechanism independent of the ODF/RANKL-RANK interaction. J Exp Med 191:275–286.
12. Teitelbaum SL. 2000. Bone resorption by osteoclasts. Science 289:1504–1508.
13. Yasuda H, Shima N, Nakagawa N, et al. 1998. Osteoclast differentiation factor is a ligand for osteoprotegerin/osteoclastogenesis-inhibitory factor and is identical to TRANCE/RANKL. Proc Natl Acad Sci USA 95:3597–3602.
14. Tsuda E, Goto M, Mochizuki S-i, et al. 1997. Isolation of a novel cytokine from human fibroblasts that specifically inhibits osteoclastogenesis. Biochem Biophys Res Commun 234:137–142.
15. Suda K, Udagawa N, Sato N, et al. 2004. Suppression of osteoprotegerin expression by prostaglandin E(2) is crucially involved in lipopolysaccharide-induced osteoclast formation. J Immunol 172:2504–2510.
16. Zou W, Bar-Shavit Z. 2002. Dual modulation of osteoclast differentiation by lipopolysaccharide. J Bone Miner Res 17:1211–1218.
17. Kikuchi T, Matsuguchi T, Tsuboi N, et al. 2001. Gene expression of osteoclast differentiation factor is induced by lipopolysaccharide in mouse osteoblasts via Toll-like receptors. J Immunol 166:3574–3579.
18. Suda K, Woo JT, Takami M, et al. 2002. Lipopolysaccharide supports survival and fusion of preosteoclasts independent of TNF-alpha, IL-1, and RANKL. J Cell Physiol 190:101–108.
19. Parfitt AM, Drezner MK, Glorieux FH, et al. 1987. Bone histomorphometry: standardization of nomenclature, symbols, and units. Report of the ASBMR Histomorphometry Nomenclature Committee. J Bone Miner Res 2:595–610.
20. Tsuji K, Kraut N, Groudine M, et al. 2001. Vitamin D(3) enhances the expression of I-mfa, an inhibitor of the MyoD family, in osteoblasts. Biochim Biophys Acta 1539:122–130.
21. Ehrlich S, Infante-Duarte C, Seeger B, et al. 2003. Regulation of soluble and surface-bound TRAIL in human T cells, B cells, and monocytes. Cytokine 24:244–253.
22. Halaas O, Vik R, Ashkenazi A, et al. 2000. Lipopolysaccharide induces expression of APO2 ligand/TRAIL in human monocytes and macrophages. Scand J Immunol 51:244–250.
23. Li P, Schwarz EM, O'Keefe RJ, et al. 2004. Systemic tumor necrosis factor alpha mediates an increase in peripheral CD11bhigh osteoclast precursors in tumor necrosis factor alpha-transgenic mice. Arthritis Rheum 50:265–276.
24. Li P, Schwarz EM, O'Keefe RJ, et al. 2004. RANK signaling is not required for TNFalpha-mediated increase in CD11(hi) osteoclast precursors but is essential for mature osteoclast formation in TNFalpha-mediated inflammatory arthritis. J Bone Miner Res 19:207–213.
25. Micheau O, Tschopp J. 2003. Induction of TNF receptor I-mediated apoptosis via two sequential signaling complexes. Cell 114:181–190.
26. Pritzker LB, Scatena M, Giachelli CM. 2004. The role of osteoprotegerin and tumor necrosis factor-related apoptosis-inducing ligand in human microvascular endothelial cell survival. Mol Biol Cell 15:2834–2841.
27. Bu R, Borysenko CW, Li Y, et al. 2003. Expression and function of TNF-family proteins and receptors in human osteoblasts. Bone 33:760–770.
28. Atkins GJ, Bouralexis S, Evdokiou A, et al. 2002 Human osteoblasts are resistant to Apo2L/TRAIL-mediated apoptosis. Bone 31:448–456.

TISSUE ENGINEERING: Part A
Volume 00, Number 00, 2009

DOI: 10.1089/ten.tea.2009.0105

Original Article

Isolation of Osteogenic Progenitor Cells from Trabecular Bone for Bone Tissue Engineering

Toshitaka Yoshii, M.D., Ph.D.,[1] Shinichi Sotome, M.D., Ph.D.,[1,2] Ichiro Torigoe, M.D., Ph.D.,[1] Hidetsugu Maehara, M.D.,[1] Yumi Sugata, M.D.,[1] Tsuyoshi Yamada, M.D.,[1] Kenichi Shinomiya, M.D., Ph.D.,[1,3,4,5] and Atsushi Okawa, M.D., Ph.D.[1]

Trabecular bone fragments can be percutaneously harvested from the ilium using methods that are similar in invasiveness to aspiration of bone marrow. In this study, we investigated the use of the trabecular bone as a cell source for bone tissue engineering. Trabecular bone-derived progenitor cells (TB cells) were isolated with a simple method in which trabecular fragments were first cultured as explants, and then the cells were released by trypsin digestion and advanced to a monolayer culture. The properties of TB cells prepared in this procedure were compared with bone marrow-derived progenitor cells (BM cells). A large number of TB cells could be obtained with less variation among donors, compared with BM cells. In multiple harvests of donor tissue through the same aspiration hole at the cortex, TB cells could be more consistently obtained in primary culture. The proliferative potential of BM and TB cells was similar in serial subculture. TB cells showed a higher alkaline phosphatase expression in the surface marker analysis and greater *in vitro* osteogenic abilities than BM cells after the initial 14 days of culture. In *in vivo* bone formation studies, TB cells also showed a higher osteogenic potential than BM cells. The results of this study suggest that TB cells can be considered an attractive source for clinical bone regeneration.

Introduction

In the orthopedic field, the use of autologous bone grafting remains the clinical practice standard of care for bone tissue repair and regeneration. However, bone grafting is limited in terms of the availability of graft material and donor site morbidity.[1] An alternative approach to the treatment of bone defects is to utilize inherent progenitor cells by transplanting them with appropriate carrier materials.[2–5]

Bone marrow-derived progenitor cells (BM cells) are known as an attractive source for bone tissue engineering[6–8] because they can be readily obtained by simple and safe bone marrow aspiration.[9] The cellular population can be expanded many fold *in vitro* and differentiated into various mesenchymal lineages, including the osteogenic lineage.[10–12] Culture-expanded BM cells have shown bone formation capability in animal models.[13–15] However, the number of BM cells that can be obtained in primary culture is often limited in clinical feasibility. Further, the number of cells that can be obtained from a given patient decreases with age and is also greatly varied among patients.[16–18] While serial subculture of the cells may be used to obtain a greater number of cells, it can also result in a reduced osteogenic differentiation capacity of the cells.[19,20] Patient-specific cell therapy, in many cases, requires large numbers of cells to replace damaged or diseased tissue. Therefore, it is desirable to establish a reliable and reproducible means of isolating a sufficient number of progenitor cells and cultivating them effectively for clinical application.

There are increasing reports that mesenchymal stem and progenitor cells can be isolated from various adult tissues,[21–24] including trabecular bone fragments.[25–28] Several procedures have been reported to isolate multipotential progenitor cells from the trabecular bone, including explant culture of collagenase-pretreated trabecular bone,[25,27,29] explant culture of trabecular bone without initial collagenase treatment,[26] and monolayer culture of collagenase-released cells.[28] Trabecular bone fragments can be percutaneously harvested from the ilium using a biopsy needle with a level of invasiveness that is comparable to BM aspiration. In addition, the procedure to harvest trabecular fragments as pieces is less influenced by peripheral blood, whereas BM aspiration is known to be highly affected by the contamination of peripheral blood. This can decrease the yield efficiency in

[1]Section of Orthopaedic and Spinal Surgery and [2]Development Division of Advanced Orthopaedic Therapeutics, Graduate School, [3]Global Center of Excellence (GCOE) Program, International Research Center for Molecular Science in Tooth and Bone Disease, [4]Hard Tissue Genome Research Center, and [5]Core to Core Program for Advanced Bone and Joint Science, Tokyo Medical and Dental University, Chiyoda-ku, Tokyo, Japan.

generating the progenitor cells.[30–33] Therefore, we have focused on trabecular bone as a cell source for bone tissue engineering and hypothesized that trabecular fragments may offer a higher yielding efficiency of osteoprogenitor cells than BM aspirates. Meanwhile, trabecular bone-derived progenitor cells (TB cells) were originally known as a source of osteoblasts,[34–36] and thus TB cells may include a rich number of progenitor cells with high osteogenic potential. However, their osteogenic abilities in *in vivo* bone regeneration have yet to be demonstrated. Therefore, we have hypothesized that TB cells may be advantageous for bone tissue engineering and examined their abilities in *in vitro* and *in vivo* osteogenesis.

We have modified the previously described methods for isolating TB cells and developed a simple protocol in which trabecular bone fragments are first cultured as explants. The cells are then released from the trabecular surface by trypsin digestion and advanced to a monolayer culture. In this study, we have compared the properties of TB cells isolated by the presented procedure to those of BM cells, specifically in terms of the osteogenic potential as well as the yield efficiency of the cells, which is important for clinical use. We have also evaluated various methods of harvesting donor tissues to effectively obtain the oseteogenic progenitor cells for bone tissue engineering.

Materials and Methods

Collection of bone marrow aspirates and trabecular bone fragments

After obtaining informed consent, both BM aspirates and trabecular bone fragments were harvested from patients who received spine surgery at Tokyo Medical and Dental University, under a protocol approved by the institutional review board.

Bone marrow aspirates were harvested from the ilium using a Jamshidi Bone Marrow Biopsy/Aspiration Needle (Allegiance Healthcare, McGaw Park, IL) and a heparinized 20-mL syringe ($n=30$; 62.7 ± 10.8 years old; 16 men, 14 women). The needle was percutaneously advanced into the intramedullary cavity of the ilium with approximately 1 cm depth from cortex, and 3 mL of BM was aspirated. Then, the same biopsy needle was inserted into the contralateral ilium in the same way (1 cm in depth) and a trabecular bone fragment (diameter: 1 mm, length: 1 cm) was obtained (Fig. 1A). These procedures to harvest 3 mL of BM and 1 cm of trabecular fragment were considered to be equivalent in clinical invasiveness. The entire sample was quickly suspended in 20 mL of standard medium (Dulbecco's modified Eagle's medium; Sigma–Aldrich, St. Louis, MO) containing 10% fetal bovine serum (Invitrogen, Carlsbad, CA) and 1% antibiotic–antimycotic (10,000 U/mL penicillin G sodium, 10,000 μg/mL streptomycin sulfate, and 25 μg/mL amphotericin B; Invitrogen), with 200 IU sodium heparin (Mochida Pharmaceutical, Tokyo, Japan).

Various harvesting methods for BM aspirates and trabecular bone fragments

To examine the influence of the aspiration volume and harvesting method on the number of progenitor cells obtained, BM aspirates with a total volume of 9 mL were percutaneously harvested by two different methods: either 3 mL of BM was sequentially harvested three times (BM-1st,

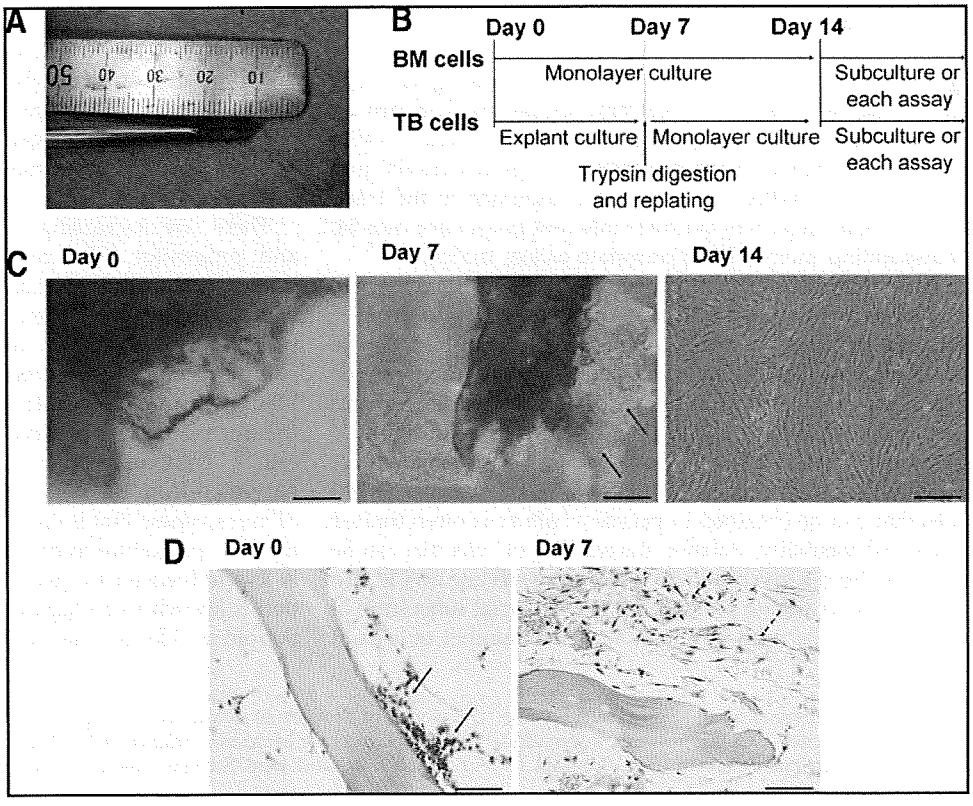

FIG. 1. (A) One-centimeter trabecular bone fragment was percutaneously harvested from the ilium using an 8-gauge biopsy needle. (B) Schematic representation of the cell culture protocol. (C) Images of explant cultures of trabecular bone fragments at days 0, 7, and 14. Arrows indicate the cells grown on the bone surface started to migrate to flask. Scale bars: 62.5 μm. (D) Representative histological sections of trabecular bone fragments at days 0 and 7 in explant culture were stained with hematoxylin and eosin. Solid arrows indicate nucleated cells on the bone surface at day 0. Dotted arrows indicate spindle-shaped cells grown on the bone surface at day 7. Scale bars: 62.5 μm. Color images available online at www.liebertonline.com/ten.

BM-2nd, and BM-3rd) from the same site by one aspiration (Fig. 2C) ($n = 10$; 59.8 ± 10.4 years old; 5 men, 5 women); or 3 mL of BM was aspirated three times, changing the direction of the needle by 45° through the same aspiration hole at the iliac crest (BM-D1, BM-D2, and BM-D3) (Fig. 2D) ($n = 5$; 56.7 ± 5.8 years old; 3 men, 2 women).[9] One-centimeter trabecular bone fragments was also harvested from the contralateral ilium three times through the same cortical hole by changing the needle direction (TB-D1, TB-D2, and TB-D3).

Culture of the cells from BM aspirates (BM cells)

The cells from BM aspirates were resuspended in the standard medium. Then, BM cells, including 1×10^7 nucleated cells, were plated in 75-cm^2 flasks (Becton, Dickinson and Company, Franklin Lakes, NJ) and were cultured with standard medium at 37°C in a humidified atmosphere containing 95% air and 5% CO_2. The medium was replaced every 3 days. After 14 days of culture, the cells were harvested with 0.25% trypsin and 1 mM ethylenediaminetetraacetic acid (EDTA; Invitrogen) for 5 min at 37°C and then counted with a hemocytometer. The cells were subsequently replated for each assay (Fig. 1B).

Culture of the cells from trabecular bone (TB cells)

One-centimeter-long trabecular bone fragments were weighed (92.2 ± 4.5 mg), cut into pieces, and washed thoroughly with phosphate-buffered saline (PBS) to remove hematopoietic cells. The fragments were then cultured as explants in the standard medium, and the medium was replaced every 3 days. At day 7, the bone fragments were digested with 0.25% trypsin and 1 mM EDTA for 10 min and replated in 75-cm^2 flasks for monolayer culture. Then, the adherent cells were harvested with 0.25% trypsin and 1 mM EDTA at day 14, counted with a hemocytometer, and subsequently replated for each assay (Fig. 1B).

Cell proliferation

The cells obtained at day 14 were replated in 75-cm^2 flasks at 2×10^3 cells/cm^2. The cells were passaged and counted with a hemocytometer every 7 days so that population doubling of the BM and TB cells could be calculated.

Colony-forming unit assay

Colony-forming unit assays were performed with BM cells (BM1, BM2, and BM3). Ten million nucleated cells were plated on a 100-mm dish and maintained in the standard medium for 7 days to form single-cell–derived colonies. Then, the dishes were stained with crystal violet to identify all colonies present, and the total number of colonies was determined.[37] Colonies smaller than 2 mm in diameter were ignored.

Analysis of cell surface markers

Flow cytometric analysis of representative cell surface markers for mesenchymal cells (CD44, CD105, and CD147), hematopoietic cells (CD34), endothelial cells (CD31), and alkaline phosphatase (ALP) were conducted using a FACSCalibur instrument (Becton, Dickinson and Company). Positive expression was defined as a level of fluorescence higher than 97% of the corresponding isotype-matched control antibody.

In vitro *osteogenic differentiation*

Both BM and TB cells were replated at 4×10^3 cells/cm^2 in a 12-well culture plate for the ALP activity assay or a 100-mm culture dish for the mineralization assay and the gene expression assay. When the culture plates reached approximately 80% confluence, the culture media of both groups were changed to an osteogenic medium containing 100 nM dexamethasone, 10 mM β-glycerophosphate (Sigma–Aldrich), and 50 μg/mL ascorbic acid phosphate (Wako, Osaka, Japan). Osteogenic culture was performed for up to 10 days (ALP, gene expression assay) or for 14 days (mineralization assay). The cells were then used for each assay.

ALP activity assay

The cells were washed with PBS, lysed with 500 μL of 0.2% Triton X-100 (Sigma–Aldrich), and sonicated to destroy cell membranes. The supernatant (10 μL) was added to 100 μL of substrate buffer (10 mM disodium *p*-nitrophenylphosphate hexahydrate, 0.056 M 2-amino-2-methyl-1,3-propanediol, and 1 mM $MgCl_2$; Wako) in a 96-well plate and incubated at 37°C for 30 min. The absorbance at 405 nm of the mixture was then measured. To normalize ALP activity, DNA content was measured using the Quant-iT PicoGreen dsDNA Assay kit (Molecular Probes, Eugene, OR) according to the manufacturer's instructions. Fluorescence intensity was measured at emission and excitation wavelengths of 516 and 492 nm, respectively.

Mineralization assay

Mineralization capability was assayed by von Kossa staining at 14 days of osteogenic induction. The cells were washed with 10 mM PBS and fixed with 10% neutral buffered formalin for 10 min. After fixation, cells were washed with 0.1 mol/L cacodylic buffer (Wako), and then 3% silver nitrate solution (Wako) was added and irradiated with UV light for 1 h. Finally, the dishes were rinsed with distilled water and air dried. BM cells without osteogenic induction served as a negative control.

RNA isolation, real-time reverse transcriptase–polymerase chain reaction

Total RNA was isolated from the culture dish using TRIZOL reagent (Invitrogen), and first strand cDNA was prepared using the Superscript III First-strand synthesis system (Invitrogen). Quantification of gene expression for runt-related gene 2/core binding factor α1 (Cbfa1), ALP, and osteocalcin (OCN) was performed by real-time polymerase chain reaction using SYBR® Premix Ex Taq™ (Takara Bio, Otsu, Japan) and Mx3000P® QPCR System (Stratagene, La Jolla, CA). β-Actin was used to normalize the amount of template present in each sample. The primer pairs used were as follows: Cbfa1 forward, 5′-GAAGGAAAGGGAGGAGGGGT; reverse, 5′-TCTGTCTCTCCT TCCCTT CC-3′; ALP forward, 5′-GAC TGGTACTCGGATAACGA-3′; reverse, 5′-TGCGGTTCCAGA CATAGTGG-3′; OCN forward, 5′-CCCAGGCGCTACCTGT ATCAA-3′; reverse 5′-GGTCAGCCAACTCGTCACAGTC-3′;

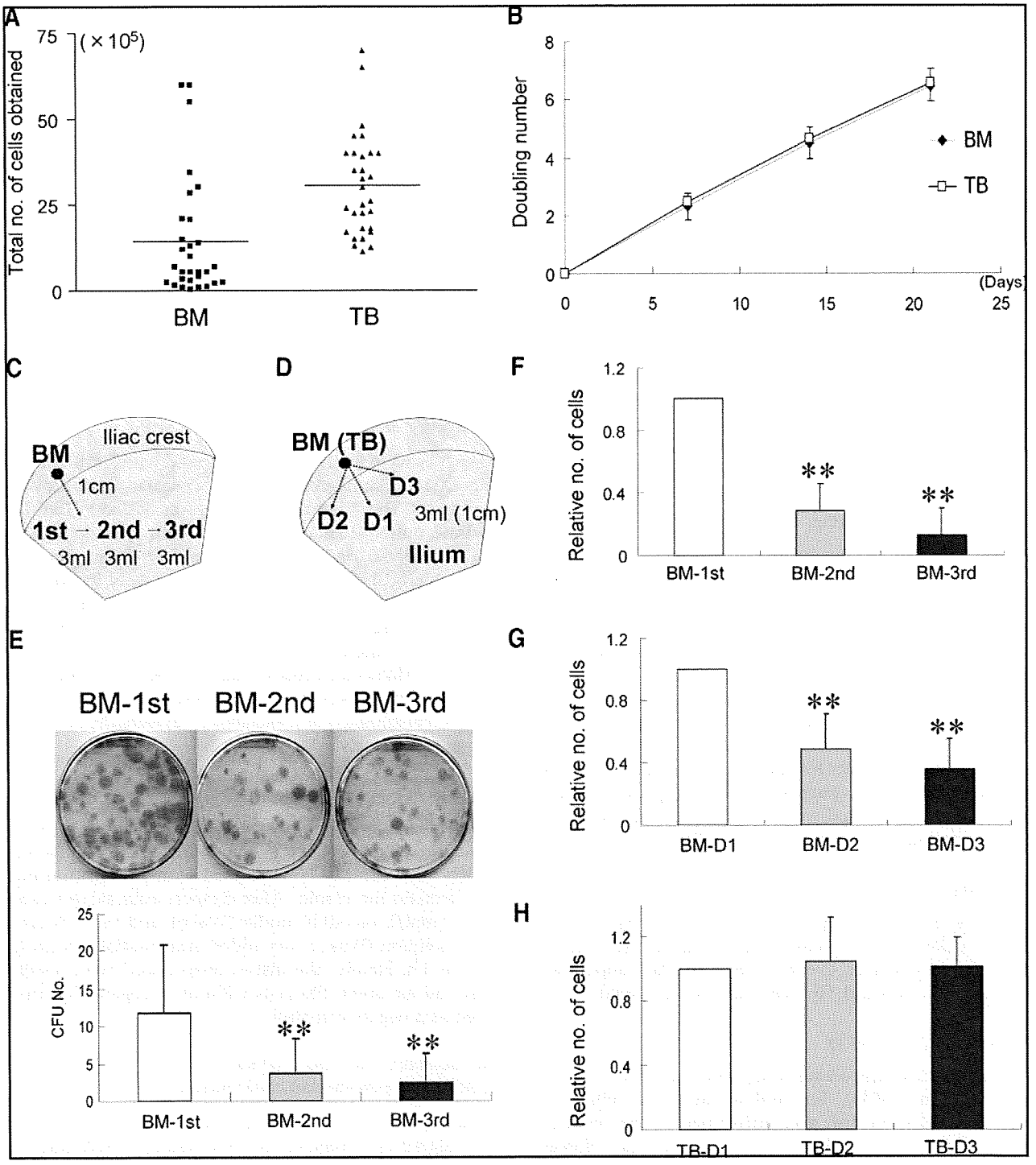

FIG. 2. (**A**) The total number of progenitor cells obtained from 3 mL of bone marrow (BM) and 1-cm trabecular bone fragment after 14 days of culture. The bar in the graph shows an average number. (**B**) Total doubling number of BM-derived progenitor cells (BM cells) and trabecular bone-derived progenitor cells (TB cells) after initial 14 days of culture. The cells were replated at 10^4 cells/cm^2 every 7 days. (**C–H**) Harvesting methods of BM and trabecular fragments: (**C**) 3 mL of BM was sequentially harvested three times (BM-1st, BM-2nd, and BM-3rd) from the same site by one aspiration; (**D**) 3 mL of BM was aspirated three times, changing the direction of the needle by 45° through the same aspiration hole at the cortical bone (BM-D1, BM-D2, and BM-D3), and 1-cm trabecular fragments were harvested in the same way from the contralateral ilium (TB-D1, TB-D2, and TB-D3); (**E**) the number of colony-forming units as determined by crystal violet staining in BM-1st, BM-2nd, and BM-3rd cells; (**F**) the number of BM-1st, BM-2nd, and BM-3rd cells; (**G**) The number of BM-D1, BM-D2, and BM-D3 cells; and (**H**) the number of TB-D1, TB-D2, and TB-D3 cells obtained at day 14. The data are expressed as mean ± standard deviation (SD) (**$p < 0.01$). Color images available online at www.liebertonline.com/ten.

β-actin forward, 5′-ATTGCCGACAGGATGCAGA-3′; reverse, 5′-GAGTACTTGCGCTCAGGAGGA-3′.

In vivo *osteogenesis (transplantation to nude mice)*

The *in vivo* osteogenic ability of the BM and TB cells was examined in a subcutaneous transplantation model using male BALB/cAJcl-*nu/nu* mice (Clea Japan, Tokyo, Japan), aged 8 weeks. All animal experiments were conducted according to the guidelines of our facility for the care and use of laboratory animals. BM and TB cells were obtained from five donors (56.7 ± 5.8 years old; 3 men, 2 women), cultured in the standard medium for 14 days according to the protocols described earlier, and replated. After 4 days of subculture with osteogenic medium, the cells were suspended in the standard medium (2×10^6 cells/mL) and used for transplantation. Implants were prepared according to the previous reports.[38,39] Cell seeding was conducted using a modified low-pressure method. Briefly, porous β-tricalcium phosphate (β-TCP) (2×2×2 mm, 75% porosity; Olympus, Tokyo, Japan) blocks were placed in an air-tight glass chamber. The air in the chamber was removed by a syringe to create low-pressure environment prior to cell seeding. Subsequently, the cell suspension was slowly infused into the chamber under low-pressure condition, and the blocks were soaked in the suspension. Then, the valve was released so that the pressure in the chamber normalized.[39] The blocks were incubated at 37°C for 6 h and were then used as implants. The mice were anesthetized by intraperitoneal administration of chloral hydrate (300 mg/kg). Four implants, either with BM or TB cells, were transplanted subcutaneously into the backs of the mice. These implants were harvested 6 weeks after implantation and fixed with 10% neutral buffered formalin. Then, these implants were decalcified with K-CX solution (Falma, Tokyo, Japan), dehydrated, embedded in paraffin, and sectioned at 5 μm thickness. The ectopic bone formation ratio for the four samples was evaluated. Modifying the report by Dennis *et al.*,[40] the newly formed bone matrix was highlighted using image-editing software (Photoshop; Adobe Systems, Inc., San Jose, CA) and measured using image-analysis software (Scion Image; Scion Corporation, Frederick, MD). The bone formation area was defined as the ratio of newly formed bone per whole sectional area including newly formed bone, pores, and β-TCP, as previously described.[39,41]

Statistics

Average values were expressed as the mean ± standard deviation. Paired *t*-test and repeated analysis of variance were used to calculate differences. Tukey–Kramer test was used for multiple comparisons. Differences were considered statistically significant when the *p*-value was <0.05.

Results

Culture of TB cells

During the initial explant culture of trabecular bone fragments in flasks, a massive amount of cell growth on the trabecular surface was observed under the microscope. At around day 7, these growing cells began to migrate onto the flask (Fig. 1C). After trypsin digestion of the bone fragments at day 7, the cells were replated into flasks, where they continued to grow efficiently as a monolayer culture. Most of the TB cells were spindle shaped, similar to BM cells, and some of the cells were polygonal shaped (Fig. 1C). While a small number of nucleated cells were observed around the trabecula on histological analysis prior to explant culture, substantial spindle-shaped cell growth was observed on the bone surface at day 7 (Fig. 1D).

Number of progenitor cells obtained

For consideration of the clinical use of the progenitor cells, the total number of cells obtained from a fixed amount of BM aspirate (3 mL) or a trabecular bone fragment of fixed size (1 cm in length) was evaluated. The average number of BM cells obtained from 3 mL of BM aspirate and TB cells obtained from 1 cm of trabecula after 14 days of culture was approximately 1.4 and 3 millions, respectively (Fig. 2A). The variation among the donors was much greater in the BM cells (60-fold difference) than in the TB cells (6.2-fold difference). Importantly, more than 1 million TB cells could be obtained from all donors. On the other hand, more than 1 million BM cells could be obtained from only half of the donors.

Proliferative ability

After 14 days of primary culture, the proliferative ability of BM and TB cells under the same culture conditions was examined. There were no significant differences in doubling number between BM and TB cells (Fig. 2B). The average doubling time was 3.3 days for BM cells and 3.2 days for TB cells.

Various harvesting methods for BM aspirates and trabecular bone fragments

At first, the influence of aspiration volume on the number of BM cells obtained was examined by collecting 3 mL of BM aspirate three times (BM-1st, BM-2nd, and BM-3rd; total 9 mL) from the same site (Fig. 2C). The number of initial nucleated cells in BM-2nd and BM-3rd was decreased more than twofold compared with that in BM-1st (data not shown). The colony-forming efficiency was also significantly decreased in BM-2nd and BM-3rd, as was the total number of cells obtained at 14 days, compared with BM-1st (Fig. 2E, F). Despite changing the direction of the needle inserted through the same cortical hole at the iliac crest to collect the BM aspirates at different sites (Fig. 2D), the number of cells that was obtained at day 14 also decreased after the initial 3 mL of aspiration (Fig. 2G). On the other hand, the total number of cells obtained from 1-cm trabecular bone fragments was maintained, even when harvested multiple times from the same cortical hole (Fig. 2H).

Surface marker profile

We examined surface epitopes of the BM and TB cells after 14 days of primary culture (Fig. 3). Both the BM and TB cells were negative for hematopoietic and endothelial markers. There were also no obvious differences between the BM and TB cells with respect to the positive surface markers of mesenchymal stem cells, CD44, CD105, and CD147. However, TB cells showed a higher positive rate for ALP than BM cells.

In vitro *osteogenic differentiation ability*

The *in vitro* osteogenic differentiation ability of the BM and TB cells was examined under osteogenic culture conditions. Cells were used after 14 days of primary culture, and ALP activity was higher in TB cells than in BM cells (Fig. 4A). However, there were no significant differences when using the cells after 28 days of culture. Interestingly, the ALP activity decreased in both BM and TB cells with further cultivation. The mineralization assay was conducted using the cells after 14 days of primary culture. TB cells showed good mineralization ability at 14 days of osteogenic induction (Fig. 4B), whereas the mineralization in BM cells was relatively limited at this time point. In the gene expression analyses after 14 days of primary culture, TB cells showed higher expression of all osteogenic markers before the cells were treated with osteogenic medium (Fig. 4C). There were no significant differences observed in Cbfa1 expression after osteogenic induction. However, TB cells showed higher ALP expression than BM cells at 5 days after starting osteogenic induction, and higher OCN expression at 5 and 10 days.

In vivo *osteogenesis*

We examined *in vivo* osteogenic potential using a subcutaneous ectopic bone formation model in athymic mice. Both the TB and BM cells were combined with porous β-TCP scaffolds and transplanted into the backs of mice. In the

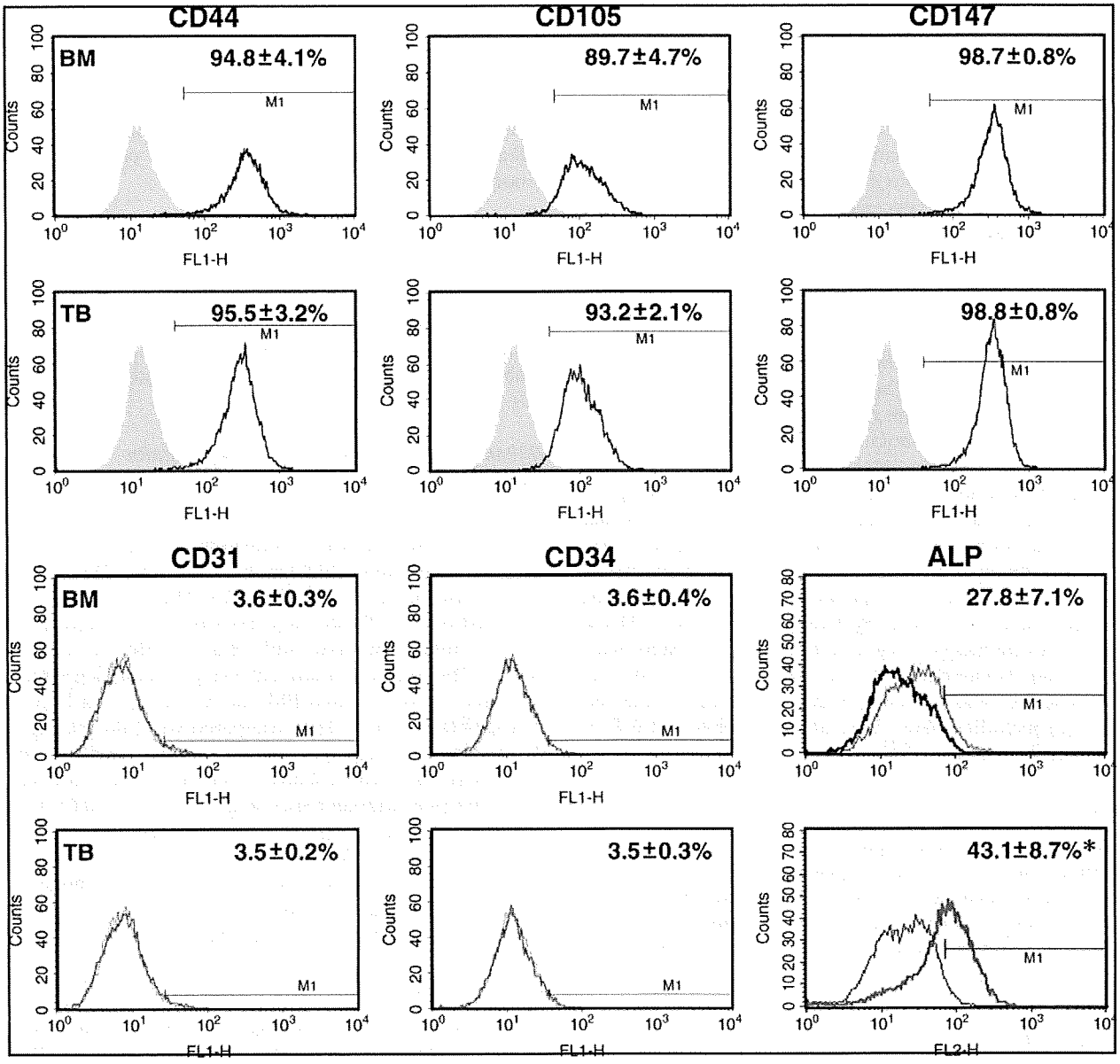

FIG. 3. Surface marker profiles. Cell surface markers in BM and TB cells were analyzed using flow cytometry. Positive expression was defined as a level of fluorescence higher than 97% of the corresponding isotype-matched control antibodies. A positive expression rate is displayed as mean ± SD. (CD44, 105, 147; shadow, isotype conntrol. CD31, 34, ALP; black line, isotype control.) Both BM and TB cells were negative for hematopoietic and endothelial markers and positive for mesenchymal markers. In alkaline phosphatase (ALP) expression, TB cells showed a higher positive rate than BM cells (*$p < 0.05$). Color images available online at www.liebertonline.com/ten.

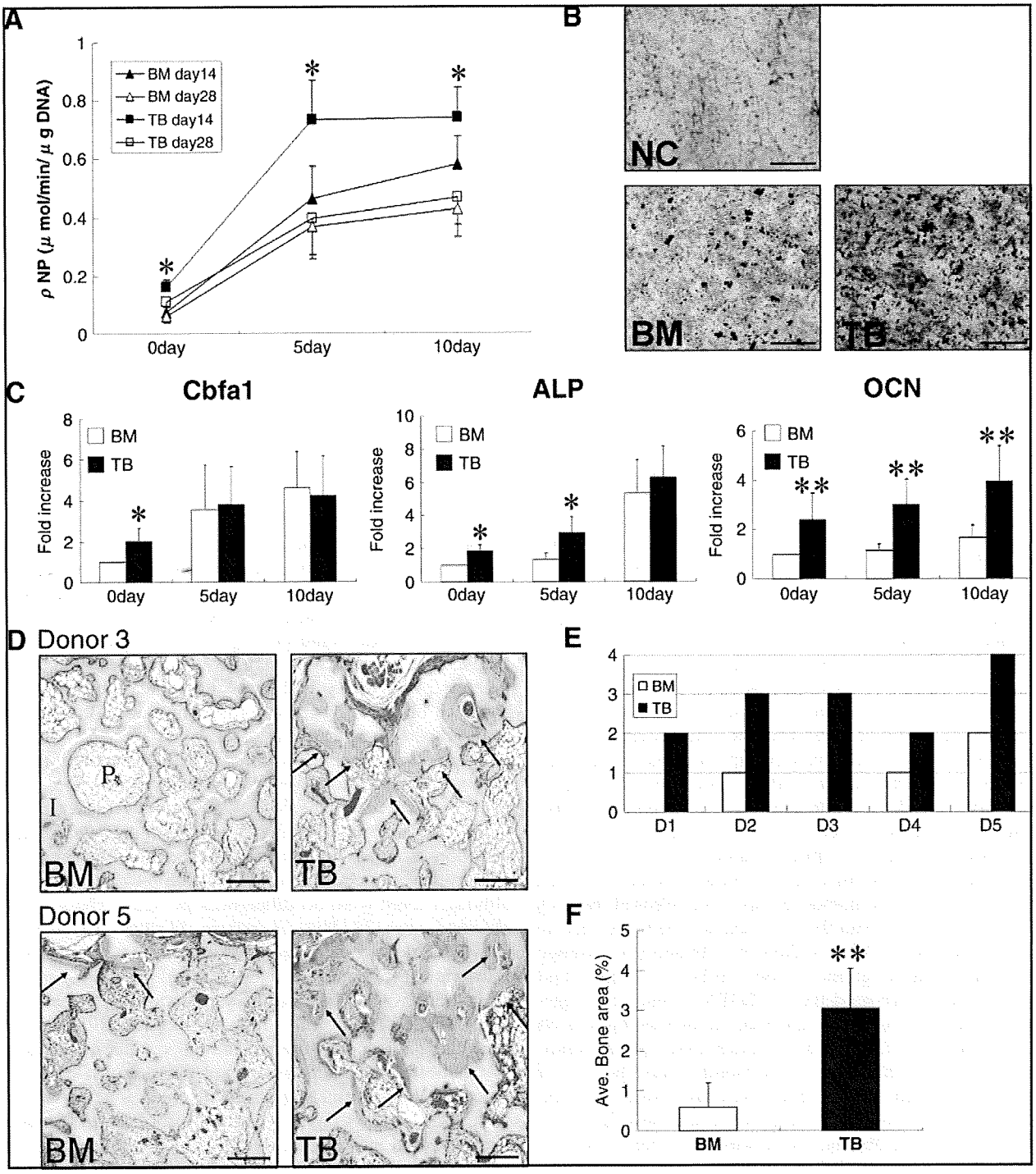

FIG. 4. *In vitro* osteogenic differentiation. (**A**) ALP activity was measured in BM and TB cells cultured for 14 or 28 days before the assay ($n = 10$). (**B**) Mineralization assay (von Kossa staining) at 14 days of osteogenic induction. NC:BM cells without osteogenic induction served as a negative control. Scale bars: 250 μm. (**C**) Quantitative analysis of mRNA expression of osteogenic markers ($n = 5$): core binding factor α1 (Cbfa1), ALP, and osteocalcin (OCN). *In vivo* bone formation analysis at an extra-skeletal site in nude mice. (**D**) Representative histological specimens from two donors stained with hematoxylin and eosin. I, implant; P, pore. Arrows indicate newly formed bone. Scale bars: 250 μm. (**E**) Total number of samples that showed ectopic bone formation in each donor (D1–5: donors 1–5). (**F**) Quantification of bone formation area in the material. The average of bone formation area per implant area is shown. The data are expressed as mean ± SD (*$p < 0.05$, **$p < 0.01$). Color images available online at www.liebertonline.com/ten.

histological analyses of the samples at 5 weeks after transplantation, a greater amount of ectopic bone formation was observed in the implants generated from TB cells than those from BM cells (Fig. 4D). For all donors, the number of implants that showed ectopic bone formation was higher when TB cells were used (Fig. 4E). Further, the average bone formation area was also greater when TB cells were used (Fig. 4F).

Discussion

Recently, Noth *et al.*[25] and Tuli *et al.*[27,29] have shown that the cells from explant cultures of collagenase-pretreated trabecular bone fragments have a multipotential differentiation capacity. In this procedure, they initially treated trabecular bone with collagenase and removed the supernatant fraction (i.e., collagenase-released cells), and the remaining bare bone fragments were cultured as explants. In contrast, Sakaguchi *et al.*[28] conducted a monolayer culture of the collagenase-released cells. These collagenase-released cells also showed excellent proliferative ability. These findings suggest that both collagenase-released cells and the remaining cells on the bone surface could be good sources for tissue regeneration. Therefore, we cultured trabecular bone fragments as explants without initial collagenase digestion to isolate osteoprogenitor cells from trabecular bone fragments simply and effectively.

Sottile *et al.*[26] also described a method by which progenitor cells can be isolated from simple explant cultures of trabecular bone fragments. They performed explant culture of bone fragments for up to 20 days, without initial collagenase digestion, and collected the cells that spontaneously migrated from the bone to the culture dishes. However, according to our observation, despite efficient cell growth on the trabecular surface in the first week, the cells reached full confluence on the bone structure at approximately day 7. As the cell growth rate declines because of contact inhibition when cultures reach full confluence, at day 7 we released the cells by trypsin digestion from the bone and proceeded to culture them as monolayers. After 14 days of cultivation, an average of 33 million cells per gram of trabecular bone was harvested by this protocol. We used trypsin-EDTA instead of collagenase to release the cells from the bone surface, as the cells do not synthesize a collagen matrix under these culture conditions. No obvious differences were found in the efficiency of cell isolation when trypsin-EDTA was used instead of collagenase in our preliminary study (data not shown).

In this study, we obtained a sufficient number of TB cells from 1 cm of trabecula with a much less variation in numbers, when compared with BM cells obtained from 3 mL of BM aspirate. When we harvest a larger volume of BM aspirates from one site, a sufficient increase in the number of progenitor cells was not observed. This is most likely due to an increase in contamination by peripheral blood in BM aspirates,[30,31,33] and it seems that the volume of aspiration from one site should be small when BM is obtained for use as a bone graft.[32] Additionally, we tested a procedure using multiple aspirations of BM from different sites through the same cortical hole. However, this procedure was also not effective in yielding a large number of cells. The number of BM cells obtained was reduced after the initial 3 mL of aspiration. We found that the number of cells obtained was stable if we harvested BM through cortical holes distant from each other (data not shown). However, this could make a greater invasiveness for the patients. On the other hand, the number of progenitor cells obtained from trabecular fragments was maintained, even when harvested multiple times through the same cortical hole. The number of TB cells obtained could increase in proportion to the amount of trabecular fragments that we harvested. Although it is difficult to make a direct comparison of 1-cm trabecular fragments and 3 mL of BM aspirates in terms of the cell number obtained from these tissues, the differences in the yield efficiency and variation in number of BM and TB cells obtained could be significant, considering clinical application.

The efficiency of obtaining cells is of critical importance for clinical cell-based tissue engineering. When we consider the clinical use of these progenitor cells, for example, in posterolateral intertransverse process lumbar spinal fusion (one of the most common lumbar spine procedure that needs bone grafts[42]), the estimated amount of progenitor cells required for one-level fusion would be 2×10^7 cells, if 20 mL of cell suspension[43] at the standard concentration of 10^6 cells/mL[44,45] are used. From the results of our study, to prepare the enough amounts of cells by 14 days of cultivation, we need six or seven trabecular fragments (1 cm), which can be harvested through one cortical hole. On the other hand, BM aspiration from 15 different sites through different cortical holes would be required to prepare 2×10^7 cells by 14 days of cultivation. This could be associated with a greater invasiveness. Although the same number of cells could be obtained by further cultivation, it may result in a reduced osteogenic capacity of the cells.[19,20]

There were no obvious differences between BM and TB cells with respect to mesenchymal stem cell surface markers.[28,46] Importantly, the expression rate of ALP was higher in TB cells than in BM cells. The *in vitro* osteogenic differentiation assay also showed that TB cells had a higher ALP activity and mineralization ability after 14 days of culture, although there were no differences in ALP activity in cells obtained after 28 days of culture. Further, TB cells also showed a higher expression of osteogenic markers in reverse transcriptase–polymerase chain reaction analysis, especially OCN transcripts. These results support our hypothesis that TB cells include cells with a higher osteogenic differentiation potential or include more differentiated cells in the osteogenic lineage at an early time-point during cultivation.

In vivo bone formation study revealed that, when cells were used after 14 days of culture, ectopic bone formation was observed in a greater number of TB cell implants than BM cell implants. This result is consistent with the *in vitro* osteogenic differentiation capacity of BM and TB cells. Thus, *in vivo* bone formation capability would also be anticipated to be reduced if these progenitor cells were to be cultured for a longer period of time, as *in vitro* osteogenic capacity declined for both BM and TB cells after further cultivation. Therefore, for either BM or TB cells, it is important to obtain a sufficient number of cells with a high osteogenic capacity in a short cultivation period; transplants should be performed before the osteogenic potential decreases.[19,20] As we can obtain a greater number of cells from trabecular bone at an early time-point during *in vitro* culture, TB cells are considered an attractive source for bone tissue engineering. Further, trabecular bone can be obtained at the same time as BM

aspirates, without increasing surgical invasiveness. Therefore, TB cells may also be used to supplement BM cells for effective bone regeneration.

In this study, we conducted cell culture and osteogenic induction in a single condition. Further studies may be required to examine the potential of these progenitor cells in different conditions. As we focused on the yielding efficiency of TB cells and their osteogenic potential in comparison to BM cells, we have not directly compared the various methods for isolating TB cells. The protocol to isolate TB cells may need to be optimized. We focused on the osteogenic potential of TB cells. Their stem cell character, including the multipotential differentiation capacities, and their abilities of maintenance in long-term culture may need to be further evaluated.

Despite the aforementioned limitations, this study demonstrates two important findings: (1) TB fragments can generate osteoprogenitor cells more effectively and consistently, and (2) TB cells have greater osteogenic potential *in vitro* and *in vivo*, when compared with BM cells. These findings support the possibility of using TB cells in clinical bone regeneration. As trabecular bone can be percutaneously harvested with limited invasion to patients, utilizing trabecular fragments as a cell source is considered to be a safe, effective, and reliable method for eventual therapeutic application in bone reconstruction surgery.

Acknowledgments

The authors thank Satoko Sunamura for excellent technical assistance, Miyoko Ojima for expert help with histological analysis, Akimoto Nimura, M.D., Ph.D., for flow cytometry analysis, Hiroshi Watanabe, M.D., Ph.D. for contribution to revision of the manuscript, and Olympus for kindly donating the porous β-TCP blocks. This work was supported by the Japan Society for the Promotion of Science, a grant-in-aid for scientific research.

Disclosure Statement

No competing financial interests exist.

References

1. Younger, E.M., and Chapman, M.W. Morbidity at bone graft donor sites. J Orthop Trauma **3,** 192, 1989.
2. Ohgushi, H., and Caplan, A.I. Stem cell technology and bioceramics: from cell to gene engineering. J Biomed Mater Res **48,** 913, 1999.
3. Bianco, P., Riminucci, M., Gronthos, S., and Robey, P.G. Bone marrow stromal stem cells: nature, biology, and potential applications. Stem Cells **19,** 180, 2001.
4. Mauney, J.R., Volloch, V., and Kaplan, D.L. Role of adult mesenchymal stem cells in bone tissue engineering applications: current status and future prospects. Tissue Eng **11,** 787, 2005.
5. Cancedda, R., Giannoni, P., and Mastrogiacomo, M. A tissue engineering approach to bone repair in large animal models and in clinical practice. Biomaterials **28,** 4240, 2007.
6. Connolly, J., Guse, R., Lippiello, L., and Dehne, R. Development of an osteogenic bone-marrow preparation. J Bone Joint Surg Am **71,** 684, 1989.
7. Muschler, G.F., Nitto, H., Matsukura, Y., Boehm, C., Valdevit, A., Kambic, H., Davros, W., Powell, K., and Easley, K. Spine fusion using cell matrix composites enriched in bone marrow-derived cells. Clin Orthop Relat Res **407,** 102, 2003.
8. Yoshii, T., Sotome, S., Torigoe, I., Tsuchiya, A., Maehara, H., Ichinose, S., and Shinomiya, K. Fresh bone marrow introduction into porous scaffolds using a simple low-pressure loading method for effective osteogenesis in a rabbit model. J Orthop Res **27,** 1, 2009.
9. Muschler, G.F., Nakamoto, C., and Griffith, L.G. Engineering principles of clinical cell-based tissue engineering. J Bone Joint Surg Am **86-A,** 1541, 2004.
10. Prockop, D.J. Marrow stromal cells as stem cells for nonhematopoietic tissues. Science **276,** 71, 1997.
11. Pittenger, M.F., Mackay, A.M., Beck, S.C., Jaiswal, R.K., Douglas, R., Mosca, J.D., Moorman, M.A., Simonetti, D.W., Craig, S., and Marshak, D.R. Multilineage potential of adult human mesenchymal stem cells. Science **284,** 143, 1999.
12. Dennis, J.E., and Charbord, P. Origin and differentiation of human and murine stroma. Stem Cells **20,** 205, 2002.
13. Bruder, S.P., Kraus, K.H., Goldberg, V.M., and Kadiyala, S. The effect of implants loaded with autologous mesenchymal stem cells on the healing of canine segmental bone defects. J Bone Joint Surg Am **80,** 985, 1998.
14. Bruder, S.P., Kurth, A.A., Shea, M., Hayes, W.C., Jaiswal, N., and Kadiyala, S. Bone regeneration by implantation of purified, culture-expanded human mesenchymal stem cells. J Orthop Res **16,** 155, 1998.
15. Petite, H., Viateau, V., Bensaid, W., Meunier, A., de Pollak, C., Bourguignon, M., Oudina, K., Sedel, L., and Guillemin, G. Tissue-engineered bone regeneration. Nat Biotechnol **18,** 959, 2000.
16. Nishida, S., Endo, N., Yamagiwa, H., Tanizawa, T., and Takahashi, H.E. Number of osteoprogenitor cells in human bone marrow markedly decreases after skeletal maturation. J Bone Miner Metab **17,** 171, 1999.
17. Muschler, G.F., Nitto, H., Boehm, C.A., and Easley, K.A. Age- and gender-related changes in the cellularity of human bone marrow and the prevalence of osteoblastic progenitors. J Orthop Res **19,** 117, 2001.
18. Phinney, D.G., Kopen, G., Righter, W., Webster, S., Tremain, N., and Prockop, D.J. Donor variation in the growth properties and osteogenic potential of human marrow stromal cells. J Cell Biochem **75,** 424, 1999.
19. Coelho, M.J., Cabral, A.T., and Fernande, M.H. Human bone cell cultures in biocompatibility testing. Part I: osteoblastic differentiation of serially passaged human bone marrow cells cultured in alpha-MEM and in DMEM. Biomaterials **21,** 1087, 2000.
20. Ter Brugge, P.J., and Jansen, J.A. *In vitro* osteogenic differentiation of rat bone marrow cells subcultured with and without dexamethasone. Tissue Eng **8,** 321, 2002.
21. Zuk, P.A., Zhu, M., Ashjian, P., De Ugarte, D.A., Huang, J.I., Mizuno, H., Alfonso, Z.C., Fraser, J.K., Benhaim, P., and Hedrick, M.H. Human adipose tissue is a source of multipotent stem cells. Mol Biol Cell **13,** 4279, 2002.
22. Cao, B., Zheng, B., Jankowski, R.J., Kimura, S., Ikezawa, M., Deasy, B., Cummins, J., Epperly, M., Qu-Petersen, Z., and Huard, J. Muscle stem cells differentiate into haematopoietic lineages but retain myogenic potential. Nat Cell Biol **5,** 640, 2003.
23. Fukumoto, T., Sperling, J.W., Sanyal, A., Fitzsimmons, J.S., Reinholz, G.G., Conover, C.A., and O'Driscoll, S.W. Combined effects of insulin-like growth factor-1 and transforming growth factor-beta1 on periosteal mesenchymal cells during chondrogenesis *in vitro*. Osteoarthritis Cartilage **11,** 55, 2003.

24. Sakaguchi, Y., Sekiya, I., Yagishita, K., and Muneta, T. Comparison of human stem cells derived from various mesenchymal tissues: superiority of synovium as a cell source. Arthritis Rheum **52,** 2521, 2005.
25. Noth, U., Osyczka, A.M., Tuli, R., Hickok, N.J., Danielson, K.G., and Tuan, R.S. Multilineage mesenchymal differentiation potential of human trabecular bone-derived cells. J Orthop Res **20,** 1060, 2002.
26. Sottile, V., Halleux, C., Bassilana, F., Keller, H., and Seuwen, K. Stem cell characteristics of human trabecular bone-derived cells. Bone **30,** 699, 2002.
27. Tuli, R., Seghatoleslami, M.R., Tuli, S., Wang, M.L., Hozack, W.J., Manner, P.A., Danielson, K.G., and Tuan, R.S. A simple, high-yield method for obtaining multipotential mesenchymal progenitor cells from trabecular bone. Mol Biotechnol **23,** 37, 2003.
28. Sakaguchi, Y., Sekiya, I., Yagishita, K., Ichinose, S., Shinomiya, K., and Muneta, T. Suspended cells from trabecular bone by collagenase digestion become virtually identical to mesenchymal stem cells obtained from marrow aspirates. Blood **104,** 2728, 2004.
29. Tuli, R., Tuli, S., Nandi, S., Wang, M.L., Alexander, P.G., Haleem-Smith, H., Hozack, W.J., Manner, P.A., Danielson, K.G., and Tuan, R.S. Characterization of multipotential mesenchymal progenitor cells derived from human trabecular bone. Stem Cells **21,** 681, 2003.
30. Batinic, D., Marusic, M., Pavletic, Z., Bogdanic, V., Uzarevic, B., Nemet, D., and Labar, B. Relationship between differing volumes of bone marrow aspirates and their cellular composition. Bone Marrow Transplant **6,** 103, 1990.
31. Bacigalupo, A., Tong, J., Podesta, M., Piaggio, G., Figari, O., Colombo, P., Sogno, G., Tedone, E., Moro, F., Van Lint, M.T., Frassoni, F., Occhini, D., Gualandi, F., Lamparelli, T., and Marmont, A.M. Bone marrow harvest for marrow transplantation: effect of multiple small (2 ml) or large (20 ml) aspirates. Bone Marrow Transplant **9,** 467, 1992.
32. Muschler, G.F., Boehm, C., and Easley, K. Aspiration to obtain osteoblast progenitor cells from human bone marrow: the influence of aspiration volume. J Bone Joint Surg Am **79,** 1699, 1997.
33. Kushida, T., Inaba, M., Ikebukuro, K., Ngahama, T., Oyaizu, H., Lee, S., Ito, T., Ichioka, N., Hisha, H., Sugiura, K., Miyashima, S., Ageyama, N., Ono, F., Iida, H., Ogawa, R., and Ikehara, S. A new method for bone marrow cell harvesting. Stem Cells **18,** 453, 2000.
34. Robey, P.G., and Termine, J.D. Human bone cells *in vitro*. Calcif Tissue Int **37,** 453, 1985.
35. Beresford, J.N., Gallagher, J.A., and Russell, R.G. 1,25-Dihydroxyvitamin D3 and human bone-derived cells *in vitro*: effects on alkaline phosphatase, type I collagen and proliferation. Endocrinology **119,** 1776, 1986.
36. Gundle, R., and Beresford, J.N. The isolation and culture of cells from explants of human trabecular bone. Calcif Tissue Int **56 Suppl 1,** S8, 1995.
37. Digirolamo, C.M., Stokes, D., Colter, D., Phinney, D.G., Class, R., and Prockop, D.J. Propagation and senescence of human marrow stromal cells in culture: a simple colony-forming assay identifies samples with the greatest potential to propagate and differentiate. Br J Haematol **107,** 275, 1999.
38. Oshina, H., Sotome, S., Yoshii, T., Torigoe, I., Sugata, Y., Maehara, H., Marukawa, E., Omura, K., and Shinomiya, K. Effects of continuous dexamethasone treatment on differentiation capabilities of bone marrow-derived mesenchymal cells. Bone **41,** 575, 2007.
39. Torigoe, I., Sotome, S., Tsuchiya, A., Yoshii, T., Takahashi, M., Kawabata, S., and Shinomiya, K. Novel cell seeding system into a porous scaffold using a modified low-pressure method to enhance cell seeding efficiency and bone formation. Cell Transplant **16,** 729, 2007.
40. Dennis, J.E., Konstantakos, E.K., Arm, D., and Caplan, A.I. *In vivo* osteogenesis assay: a rapid method for quantitative analysis. Biomaterials **19,** 1323, 1998.
41. Torigoe, I., Sotome, S., Tsuchiya, A., Yoshii, T., Maehara, H., Sugata, Y., Ichinose, S., Shinomiya, K., and Okawa, A. Bone regeneration with autologous plasma, bone marrow stromal cells, and porous beta-tricalcium phosphate in nonhuman primates. Tissue Eng Part A **15,** 1489, 2009.
42. Katz, J.N. Lumbar spinal fusion. Surgical rates, costs, and complications. Spine **20,** 78S, 1995.
43. Neen, D., Noyes, D., Shaw, M., Gwilym, S., Fairlie, N., and Birch, N. Healos and bone marrow aspirate used for lumbar spine fusion: a case controlled study comparing healos with autograft. Spine **31,** E636, 2006.
44. Yoshikawa, T., Ohgushi, H., Uemura, T., Nakajima, H., Ichijima, K., Tamai, S., and Tateisi, T. Human marrow cells-derived cultured bone in porous ceramics. Biomed Mater Eng **8,** 311, 1998.
45. Dong, J., Kojima, H., Uemura, T., Kikuchi, M., Tateishi, T., and Tanaka, J. *In vivo* evaluation of a novel porous hydroxyapatite to sustain osteogenesis of transplanted bone marrow-derived osteoblastic cells. J Biomed Mater Res **57,** 208, 2001.
46. Wagner, W., Wein, F., Seckinger, A., Frankhauser, M., Wirkner, U., Krause, U., Blake, J., Schwager, C., Eckstein, V., Ansorge, W., and Ho, A.D. Comparative characteristics of mesenchymal stem cells from human bone marrow, adipose tissue, and umbilical cord blood. Exp Hematol **33,** 1402, 2005.

Address correspondence to:
Shinichi Sotome, M.D., Ph.D.
Section of Regenerative Therapeutics for Spine and Spinal Cord
Graduate School
Tokyo Medical and Dental University
1-5-45 Yushima
Bunkyo-ku, Tokyo 113-8519
Japan

E-mail: sotome.orth@tmd.ac.jp

Received: February 16, 2009
Accepted: October 14, 2009
Online Publication Date: November 24, 2009

Effects of Gamma-Ray Irradiation on Mechanical Properties, Osteoconductivity, and Absorption of Porous Hydroxyapatite/Collagen

Yuichi Kawasaki,[1] Shinichi Sotome,[1,2] Toshitaka Yoshii,[1] Ichiro Torigoe,[1] Hidetsugu Maehara,[1] Yumi Sugata,[1,3] Masahiro Hirano,[4] Naomi Mochizuki,[4] Kenichi Shinomiya,[1,3,5,6] Atsushi Okawa[1]

[1] Department of Orthopaedic and Spinal Surgery, Graduate School, Tokyo Medical and Dental University, Bunkyo-ku, Tokyo 113-8519, Japan

[2] Department of Regenerative Therapeutics for Spine and Spinal Cord, Graduate School, Tokyo Medical and Dental University, Bunkyo-ku, Tokyo 113-8519, Japan

[3] Global Center of Excellence (GCOE) Program, International Research Center for Molecular Science in Tooth and Bone Disease, Tokyo Medical and Dental University, Bunkyo-ku, Tokyo 113-8519, Japan

[4] PENTAX New Ceramics Division, HOYA Corporation, Itabashi-ku, Tokyo 174-8639, Japan

[5] Hard Tissue Genome Research Center, Tokyo Medical and Dental University, Chiyoda-ku, Tokyo 101-0062, Japan

[6] Core to Core Program for Advanced Bone and Joint Science, Tokyo Medical and Dental University, Chiyoda-ku, Tokyo 101-0062, Japan

Received 28 February 2009; revised 28 June 2009; accepted 16 July 2009
Published online 2 October 2009 in Wiley InterScience (www.interscience.wiley.com). DOI: 10.1002/jbm.b.31502

Abstract: In this study, the effects of gamma-ray irradiation on the mechanical properties, absorbability, and osteoconductivity of porous hydroxyapatite/collagen (HAp/Col) were investigated. Porous HAp/Col was exposed to 16, 25, 35, or 50 kGy of gamma-ray irradiation. The compressive elastic modulus showed irradiation dose-dependence, with a particularly pronounced decrease in the 50-kGy treatment group. An *in vitro* enzymatic digestion test showed that gamma-ray irradiation of porous HAp/Col resulted in accelerated degradation by collagenase. For *in vivo* studies, porous HAp/Col was transplanted into the back muscles or bone defects in the femoral condyle of rats. Specimens were obtained at 2, 4, and 8 weeks postoperatively. Absorption of the implants in the muscle was time- and irradiation dose-dependent, with notable absorption for the 35- and 50-kGy groups at 2 weeks. At the skeletal sites, porous HAp/Col demonstrated high osteoconductivity in all irradiation treatment groups. Interestingly, not only implant absorption but also bone formation was irradiation dose-dependent at early time points. © 2009 Wiley Periodicals, Inc. J Biomed Mater Res Part B: Appl Biomater 92B: 161–167, 2010

Keywords: gamma ray irradiation; osteoconduction; bioabsorption; hydroxyapatite composite; collagen

INTRODUCTION

Artificial bone substitutes are widely used to reconstruct bone defects caused by tumors, trauma, and other adverse events. Sintered calcium phosphates and their composites have been the materials most widely used as bone substitutes,[1–4] although a variety of composites composed of inorganic and organic materials such as hydroxyapatite/collagen (HAp/Col) have also been developed recently.

HAp/Col has a nanostructure similar to that of natural bone; it is composed of nanoscale needle-like HAp crystals with *c*-axes aligned along type I atelocollagen fibers derived from porcine skin. The HAp/Col weight ratio is 80:20.[5] Previous reports using HAp/Col implants with different macrostructures (dense or porous HAp/Col or as a composite with alginate) have demonstrated satisfactory osteoconductivity and bioabsorption when the implants were used as a bone substitute.[6–9] Above all, porous HAp/Col is a promising bone substitute for clinical use

Correspondence to: S. Sotome (e-mail: sotome.orth@tmd.ac.jp)
Contract grant sponsor: The Ministry of Education, Culture, Sports, Science and Technology of Japan

because it has a sponge-like elasticity that makes it easy to handle during surgery. It can also be used as a drug delivery carrier for bone reconstruction.[9]

For clinical implementation of HAp/Col, sterilization is necessary. However, available sterilization methods are limited because of the distinctive composition of this material. Ethylene oxide gas, one of the most popular means of sterilization, stably adsorbs onto HAp crystals because of their broad adsorptive area.[10] Autoclaving also cannot be used for HAp/Col sterilization because the high-pressure steam severely disrupts the collagen fibers while leaving HAp crystals intact.[11,12] Therefore, these common sterilization methods are inappropriate for preparing HAp/Col for clinic use.

Although gamma-ray irradiation also disrupts collagen fibers to some degree, the severity of this disruption is much lower than that caused by autoclaving.[13] However, the specific effects of gamma rays on collagen fibers or collagen-containing composites have not been established. A previous study reported that 25 kGy of gamma-ray irradiation affected not only resistance to enzymatic digestion and the porous structure of a collagen sponge but also *in vitro* cell migration into the sponge.[14] Another group reported that 15-kGy irradiation of a bone graft did not compromise its efficacy.[15] There are many other conflicting reports about the effects of gamma rays on collagen or collagen-based composites.

In this study, the effects of a variety of doses of gamma-ray irradiation on the mechanical properties, bioabsorbability, and osteoconductivity of porous HAp/Col were examined.

MATERIALS AND METHODS

Preparation of Porous Hydroxyapatite/Collagen

HAp/Col nanocomposite fibers were synthesized from a $Ca(OH)_2$ suspension and H_3PO_4 solution, which contained atelocollagen derived from porcine skin, using a previously reported coprecipitation method.[5] Briefly, 400 m*M* $Ca(OH)_2$ and 120 m*M* H_3PO_4 containing dissolved collagen (atelo-type I collagen from porcine dermis; Nitta Gelatin, Japan) were simultaneously added slowly to distilled water kept at 40°C in a water bath. The speed of the dropwise addition was controlled to maintain the pH at 9.0. The initial HAp/Col weight ratio was 80:20. The obtained HAp/Col precipitate was lyophilized and used to prepare porous HAp/Col. Next, 1 g of HAp/Col fibers was homogenized with 6.5 mL of phosphate-buffered saline (PBS) and alkalized with 50 μL of 1*M* sodium hydroxide solution. This mixture was combined with 1.5 mL of 0.6% collagen in phosphoric acid (pH 2.0). The resultant mixture (pH 7.0) was infused into a mold. To initiate gelation of collagen as a binder, the mold containing the mixture was incubated at 37°C for 2 h. Next, the gelled mixture was frozen at −60°C, allowing the remaining liquid to form ice crystals within the gel. The spaces occupied by the ice crystals were converted to pores by subsequent lyophilization. These lyophilized porous HAp/Col composites were dehydrothermally treated at 140°C for 12 h in a vacuum to introduce crosslinking of the collagen molecules. Porous HAp/Col was then cut to samples 10 mm × 10 mm × 10 mm in size for mechanical testing, 10 mm × 10 mm × 5 mm for *in vitro* bioabsorption testing, and 2 mm × 2 mm × 3 mm for *in vivo* analyses. The porous HAp/Col constructs were sterilized by gamma-ray irradiation at 16, 25, 35, or 50 kGy or treated with 70% ethanol for 10 min as a control.

Mechanical Testing

The compressive mechanical properties of porous HAp/Col with a 10 mm × 10 mm × 10 mm cubic shape were analyzed using a mechanical examination machine with a load cell capacity of 20 N, (N = 5) (EZ test-20N; Shimadzu Corporation, Japan). The specimens were moisturized by soaking in distilled water for 2 min under vacuum to remove the remaining air in the pores, causing them to become elastic and sponge-like. Each specimen was compressed perpendicularly at a cross-head speed of 10 mm/min to achieve a strain of 25% and then was immediately returned to the initial position. This cyclic test was repeated four times. The recovery rate and the compressive elastic modulus at 10 and 20% strain were calculated from the stress–strain curve of the fourth compression. After the compression test, the specimens were prepared for observation by scanning electron microscopy (SEM).

SEM Examination

After mechanical compressive testing, the specimens were fixed with 2.5% glutaraldehyde, cut at the center, and post-fixed with 0.1% osmium tetroxide. Next, the samples were dehydrated through a graded series of ethanol washes, dried by a critical point dryer, mounted onto aluminum stubs, and sputter-coated with platinum. The samples were observed from the cut plane using a SEM (Hitachi S4200 FESEM, HITACHI, Tokyo, Japan).

In Vitro Bioabsorption

The *in vitro* bioresorbability of porous HAp/Col was tested using the collagenase digestion model reported by Yunoki et al.[16] Blocks of porous HAp/Col (10 mm × 10 mm × 5 mm) with a weight of 70.3 ± 3.0 mg (mean ± SD) were immersed in 5 mL PBS containing 375 U of bacterial collagenase (*Clostridium histolyticum*; Wako Pure Chemical Industries) and incubated at 37°C for 1 (N = 3) or 2 (N = 6) h. The collagenase solution and the sediment of degraded HAp/Col were then removed using a pipette. The remaining HAp/Col blocks were frozen, freeze-dried, and weighed. The remaining weight was normalized against the initial weight by taking the percentage.

Surgical Procedures

All experimental animals used in these studies were maintained and treated according to the guidelines for the care and use of laboratory animals of the Tokyo Medical and Dental University. After anesthesia by intraperitoneal administration of 7% trichloroacetaldehyde monohydrate solution (0.5 mL per 100 g of body weight) and aseptic preparation, HAp/Col implants were transplanted into bone defects created in the distal ends of the femurs and into pouches in the back muscles of male rats (F344, age 11 weeks, weight 240–250 g). The distal end of the femur shaft was exposed by lateral approach and a 3-mm diameter hole was bored using an electric drill with continuous saline irrigation. The drill hole was then rinsed with saline, and the implant was placed in the hole. At 2, 4, and 8 weeks post-transplantation, the rats were euthanized and the femurs and composites transplanted into the back muscles were excised.

Quantification of Porous HAp/Col in Back Muscle

Porous HAp/Col implants removed from the dorsal muscle were scanned using a micro-CT scanner (ScanXmate-E090; Comscantecno, Japan) before fixation to exclude the effects of fixation on sample volume. Three-dimensional image data were then reconstructed, and the volume of the porous implant was calculated using the three-dimensional bone analysis software TRI/3D-BON (Ratoc System Engineering, Japan).

Histological Analysis

After micro-CT analysis, samples were fixed in 4% paraformaldehyde, decalcified in 20% ethylenediaminetetraacetic acid (EDTA), dehydrated using a graded alcohol series, and embedded in paraffin wax. Sections of 5-μm thickness were cut and stained with hematoxylin and eosin (HE) or tartrate-resistant acid phosphatase stain (TRAP).

Statistical Analysis

Overall differences among groups in the mechanical test were determined by two-factor repeated measures analysis of variance (ANOVA), and those in the other experiments were determined by two-factor ANOVA, and differences between individual groups were estimated using the Tukey-Kramer multiple comparison test. Differences were considered statistically significant when the p value was <0.05.

RESULTS

Compressive Mechanical Test

Swelling of the samples after rehydration was not detected by macroscopic observation. All tested samples behaved elastically, and recovery rates after the fourth compression were greater than 92% in all groups, although there was a slight irradiation dose-dependent decrease in recovery rate (Table I). Compared to the nonirradiated control, the compressive elastic modulus of all irradiated groups was markedly decreased at strains of both 10 and 20%, with the lowest modulus observed in the 50-kGy group [Figure 1(A)]. SEM images of porous HAp/Col specimens after mechanical testing demonstrated that although slight compressive deformation of the porous structures remained, there was no apparent disruption of the materials in any group, including those treated with 50-kGy irradiation [Figure 1(B)].

TABLE I. Recovery Rates of Compression Test

Control	16 kGy	25 kGy	35 kGy	50 kGy
94.3%	93.4%	93.5%	93.1%	92.8%

In Vitro Bioresorbability

Figure 2 shows the remaining weight of the HAp/Col composite after enzymatic digestion by collagenase. As the irradiation dose increased, the remaining weight decreased. The reduction ratios of the remaining porous HAp/Col in the 35- and 50-kGy groups were significantly higher than those of the other groups.

Quantification of Porous HAp/Col in Back Muscle

Figure 3 shows the volume of residual porous HAp/Col extracted from the back muscle. Control implants were scarcely absorbed until 8 weeks after transplantation. In contrast, all irradiated implants showed dose-dependent decrease in volume, with the 35- and 50-kGy irradiation-treated specimens exhibiting drastic volume decreases 2 weeks postoperatively. The average volume of the 50-kGy group was increased slightly at 4 and 8 weeks, where this may have been due to dispersion of the fragmented implant following tissue invasion.

Histological Analysis

Porous HAp/Col at the Extraskeletal Site. Fragmentation of porous HAp/Col implants and multinucleated macrophage attachment were observed in all irradiated groups at 2 weeks post-transplantation. The 50-kGy-treated implants were the most severely fragmented and reduced, with a large number of multinucleated macrophages attaching to the fragments. In the control group, despite the presence of macrophages, the porous structure of the extracted implants was maintained (Figure 4).

At 4 weeks after implantation, although the extracted implants in the 16-, 25-, and 35-kGy groups were almost completely fragmented and the original porous structures could not be recognized, the volume of the remnants of the 35- and the 50-kGy implants was still lower. Partial fragmentation of the control implant was also observed at 4 weeks postoperatively. At 8 weeks, absorption of the 25-